Geol. Mag. **150** (*6*), *2013, pp. 1062–1084.* © *Cambridge University Press 2013*
doi:10.1017/S0016756813000320

The Oligocene–Miocene tectonic evolution of the northern Outer Carpathian fold-and-thrust belt: insights from compression-and-rotation analogue modelling experiments

MARTA RAUCH*

Institute of Geological Sciences, Polish Academy of Sciences INGPAN, Research Centre in Wroclaw, Podwale 75, PL 50449 Wrocław, Poland

(*Received* 25 May 2011; *accepted* 20 March 2013; *first published online* 24 May 2013)

Abstract – This paper presents the different analogue scenarios of the tectonic evolution of the northern Outer Carpathians (i.e. the Western and northern Eastern Outer Carpathians) which formed as an accretionary wedge in front of the East Alpine–Carpathian–Pannonian (ALCAPA) block during Oligocene–Miocene times. Currently, this fold-and-thrust belt forms an arc which is asymmetrically convex to the north and wider in its eastern part. Palaeomagnetic investigations have suggested that the rocks of the arc underwent counter-clockwise rotation along almost the whole arc, which is difficult to explain as an effect of simple indentation of the triangular indenter. In this case two branches of the arc should be rotated in the opposite directions. The structural evolution of the Western Outer Carpathians is characterized by superposition of two successive tectonic shortening events directed N–S and NE–SW. The results of the presented analogue modelling suggest that two scenarios of the geodynamic evolution of the studied belt could explain the occurrence of such differently oriented shortening events: (1) two phases of differently directed indentation (first to the N, then to the NE) and (2) indenter movement to the NE with simultaneous counter-clockwise rotation. However, the experiment in which the moving indenter is simultaneously rotated produces the most suitable model. The counter-clockwise rotation of the material is only possible in front of both sides of the convex indenter in this model. The results of the analogue modelling also prove that rotation of the ALCAPA block started after formation of the Magura nappe (the innermost nappe of the Western Outer Carpathians).

Keywords: analogue modelling, rotation, arcuate belt, Outer Carpathians, Western Alps.

1. Introduction

The characteristics of fold-and-thrust belt curvature have been studied for many years via analogue modelling (e.g. Marshak & Wilkerson, 1992; Calassou *et al.* 1993; Zweigel, 1998; Macedo & Marshak, 1999; Cotton & Koyi, 2000; Lickorish *et al.* 2002; Marshak 2004; Reiter *et al.* 2011). Many different parameters have been tested, such as different curvatures of the indenter, variations in thickness within the deforming layers, variations in basal friction and irregularities in the footwall/foreland. This paper focuses on indenter-related parameters, similar to the work performed by Macedo & Marshak (1999). These parameters relate to different indenter shapes and to the various ways in which the indenter is moved. The experimental material used in the models was wet sandy silt. Special attention was paid to the influence of indenter rotation on the formation of fault patterns in front of the moving rigid indenter. Many geodynamic reconstructions have postulated a rotation of the advancing crustal block: for example, an anticlockwise rotation of the Adria block (Western Alps) during the Miocene (Vialon *et al.* 1989); a clockwise rotation of the Tarim block (Western Himalaya) during the Devonian (e.g. Chen *et al.* 1999) and an anticlockwise rotation of the Iberian plate during the Late Cretaceous (O'Brien, 2001).

The aim of the present investigation is to determine a plausible geodynamic analogue scenario for the Oligocene–Miocene tectonic evolution of the northern Outer Carpathian fold-and-thrust belt. The Outer Carpathians are an external part of the Carpathian–Pannonian–Dinaride system (Fig. 1; e.g. Csontos & Vörös, 2004; Schmid *et al.* 2008). Current opinion suggests that the northern Outer Carpathian belt, i.e. the Western and northern Eastern Carpathians, formed in front of the advancing East Alpine–Carpathian–Pannonian (ALCAPA) block (which is a continental fragment) as an accretionary prism from Oligocene time (e.g. Pescatore & Ślączka 1984; Morley 1996; Behrmann *et al*. 2000) up to the Middle Miocene (the Serravallian, locally termed the Sarmatian; e.g. Oszczypko, 2006; Nemčok *et al.* 2007). Based on the results of these investigations, the ALCAPA block may be a key element in formation of the Outer Carpathian fold-and-thrust belt. This belt developed in front of the ALCAPA block which could behave as a huge bulldozer (for explanation see Chapple, 1978). Moreover, the southern boundary of the northern Outer Carpathians is quasi-triangular in outline and concave northerly. The northern outline of the northern Outer Carpathians is convex to the north and slightly mimics the arcuate shape of the southern boundary. What

*E-mail: ndrauch@cyf-kr.edu.pl

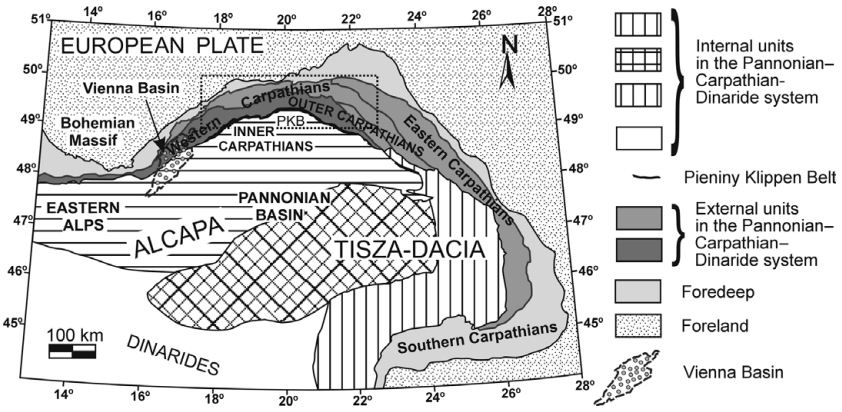

Figure 1. Map of the Carpathian–Pannonian–Dinaride system (Csontos *et al.* 1992) with location of the Vienna basin (Kováč *et al.* 1998). The rectangle marks the most northern part of the northern Outer Carpathians, the location of the Polish part of Carpathians shown in Figure 2a. Geology of the Polish Carpathians modified after Książkiewicz (1977) and Jankowski (1997). PKB: Pieniny Klippen Belt.

may confirm the movement of the triangular indenter, which is an equivalent of the ALCAPA block, is the construction of an analogue model of the northern Outer Carpathian fold-and-thrust belt. The influence of indenter-controlled parameters on the generation of curved fold-and-thrust belts is indisputable (Macedo & Marshak, 1999). Therefore, this effect is first explored in modelling the tectonic development of the northern Outer Carpathians.

To date, there have been four publications that have analogue modelled the geodynamic evolution of the Outer Carpathians. In modelling the Eastern Carpathians, Zweigel (1998) modelled the influence of the shape of the upper plate and the movement direction of the upper plate relative to the orientation of its margins. In their investigation of the Western Outer Carpathians, Nemčok *et al*. (1999) used the results of the model examining the influence of basal friction on thrust generation. Rauch (2001) extended the results of Zweigel (1998) by testing indenter-controlled parameters on the modelled evolution of the Western Outer Carpathians. Sieniawska *et al*. (2010) modelled a fragment of the Polish Carpathian orogenic front and tested the influence of synorogenic sedimentation in front of an active fold-and-thrust wedge that rested on top of a weak ductile detachment horizon, thereby examining the dynamics of growth structures.

The results of the experiments presented in this paper are the first modelling of the tectonic evolution of the entire northern Outer Carpathians. The most northern segment of the northern Outer Carpathians is located in Poland. The Polish part of the northern Outer Carpathians occupies a significant geological position: it occurs in front of the apex formed by the Pieniny Klippen Belt which is the border between the Outer and Inner Carpathians. The latter belongs to the ALCAPA block, and provides the possibility of studying the influence of the advancing ALCAPA block on the formation of the Carpathian accretionary prism.

2. Regional background

2.a. Alpine–Carpathian–Pannonian System

The Outer Carpathian arc (Fig. 1) is the external part of the Carpathian orogen and is characterized by outward-verging nappes. Mapping of the Carpathian–Pannonian region suggests that there are two distinct crustal blocks here, named microplates or mega-units. These have been termed the Alpine–Carpathian–Pannonian (ALCAPA) block and Tisza–Dacia block (e.g. Fodor *et al.* 1999; Csontos & Vörös, 2004; Schmid *et al.* 2008). The two parts of the composite Tisza–Dacia block are considered as independent terranes in the Mesozoic (Csontos & Vörös 2004). The ALCAPA and Tisza–Dacia blocks moved as two separate crustal fragments during the development of the Outer Carpathian arc (e.g. Csontos, 1995; Fodor *et al.* 1999). According to Csontos & Vörös (2004), the ALCAPA block includes the Eastern Alps, West Carpathians and Transdanubian Range north of Lake Balaton.

The overall driving mechanism for the development the Carpathian area was the convergence of Africa with Europe (e.g. Dewey *et al.* 1973; Burchfil, 1980; Royden, 1993; Golonka *et al.* 2000; Neugebauer *et al.* 2001). The migration of the ALCAPA and Tisza–Dacia blocks towards their present location in the Carpathian realm was accompanied by an eastwards extrusion in the Eastern Alps (Ratschbacher *et al.* 1991*a*, *b*), by an eastwards retreat of European crust (Royden & Burchfield, 1989; Royden, 1993; Nemčok *et al.* 2006) and by eastwards migration of the last collisional activity along the Carpathian arc (e.g. Nemčok *et al.* 2006). Lateral extrusion in the Eastern Alps, forced by the continental collision which affected the Alps, was possible because the subduction retreat provided the space necessary for this eastwards movement (Ratschbacher *et al.* 1991*a*; Sperner *et al.* 2002). A continental escape of the ALCAPA block from the Alpine area started in the Late Eocene (Fodor

https://doi.org/10.1017/S0016756813000320 Published online by Cambridge University Press

et al. 1992), but best developed in the Oligocene (Csontos *et al.* 1992; Fodor *et al.* 1992). The amount of this escape is estimated as *c.* 60–100 km in the Alps (Schmid *et al.* 1989). According to Frisch *et al.* (1998), the lateral extrusion of the Eastern Alpine units lasted from the late Late Oligocene to the late Middle Miocene. Starting in the late Early Miocene, crustal deformation in the Carpathian realm was characterized by the mutually opposite rotation of the ALCAPA and Tisza–Dacia blocks and their progressive advancement into the Carpathian embayment (e.g. Balla 1987). The northern part of the Outer Carpathian belt – the Western and northern part of the Eastern Carpathians – formed in front of the advancing ALCAPA block during Late Eocene – Middle Miocene times (Nemčok *et al.* 2007). The thrusting in the East Outer Carpathians continued into the Early Pliocene (Late Miocene; Matenco & Bertotti, 2000).

During the last two decades, numerous kinematic or palinspastic restorations of the Alpine–Carpathian–Dinaride system have been published (e.g. Balla, 1987; Csontos *et al.* 1992; Kováč *et al.* 1994; Nemčok *et al.* 1998*a*; Fodor *et al.* 1999; Márton *et al.* 2000; Ustaszewski *et al*. 2008). Certain reconstructions of the Neogene evolution of the ALCAPA region have suggested that there was a very important 30–90° counter-clockwise rotation of the ALCAPA block (e.g. Balla, 1987; Márton & Márton, 1996; Fodor *et al.* 1999), while others have considered ALCAPA rotation to be minor (e.g. Ustaszewski *et al.* 2008) or absent (e.g. Ellouze & Roca, 1994). The amount of the Neogene counter-clockwise rotation of the ALCAPA block is still an open question. Based on palaeomagnetic observation, it could be 30–35° (Balla, 1987), 80° (Márton *et al.* 2007) or even 70–90° (Márton & Márton, 1996; Fodor *et al.* 1999).

The northern Outer Carpathians (the Western and the most northern part of Eastern Outer Carpathians) are located close to the ALCAPA block (Fig. 1). Past research has supported the idea that the ALCAPA block has played a significant role in the formation of the northern Outer Carpathian belt (e.g. Kováč *et al.* 1994; Fodor *et al.* 1999; Nemčok *et al.* 1998*a*, *b*).

2.b. Western Outer Carpathians as the main part of the northern Outer Carpathians

The Western Carpathians and the most northern part of Eastern Carpathians (Fig. 1) have traditionally been divided into two ranges by the Pieniny Klippen Belt: an older, inner range and a younger, outer range (Książkiewicz, 1977). The West Inner Carpathians represent a Late Cretaceous imbricated nappe system comprising crystalline basement units and post-nappe Late Cretaceous – Neogene sedimentary and volcanic formations (e.g. Książkiewicz, 1977; Plašienka, 1991; Plašienka *et al.* 1997; Lexa *et al.* 2003).

The Pieniny Klippen Belt is *c.* 600 km long and is now a 1–20-km-wide shear zone (Książkiewicz, 1977; Birkenmajer, 1986; Nemčok & Nemčok, 1994). This belt comprises Mesozoic and Palaeogene rocks that were once a nappe pile but that were subsequently intensely deformed in a shear zone (Książkiewicz, 1977; Birkenmajer, 1986; Ratschbacher *et al.* 1993; Nemčok & Nemčok, 1994). The belt became a shear zone during the Miocene (e.g. Nemčok & Nemčok, 1994).

The Polish segment of the northern Outer Carpathians (Fig. 2a) is a north-verging fold-and-thrust belt (Fig. 2b) composed of Upper Jurassic – Lower Miocene flysch-dominated rocks (Książkiewicz, 1977; Oszczypko, 2004; Ślączka *et al.* 2005). The belt comprises five nappe complexes (from south to north): the Magura, the Fore-Magura–Dukla Group, the Silesian, the Subsilesian and the Skole (Fig. 2a). Only the most southern nappe, which is called Magura, extends along the whole Western Outer Carpathians. The other nappes are exposed mostly in the central and eastern part of the Western Outer Carpathians. The only exception is the Subsilesian nappe along with its western equivalents (Ždánice and Waschberg units), which crop out more extensively in the western part of Western Outer Carpathians (Picha *et al.* 2005). The Miocene sediments of the southern part of the Polish Carpathian Foredeep were also deformed and incorporated into the Western Outer Carpathians as the Zgłobice Unit (Kotlarczyk, 1985; Krzywiec, 2001). Sedimentation in the Carpathian Foredeep lasted to the Middle Miocene (the Serravallian, locally termed the Sarmatian; Oszczypko, 1998), but the presence of the Pannonian sediments (Olszewska, 1999; Wójcik *et al.* 1999) suggests that sedimentation could have finished as late as 8 Ma (Late Miocene; according to B. Olszewska in Márton *et al.* 2011). The Carpathian Foredeep sediments were deposited on the highly complex epi-Variscan platform and on the Permian–Mesozoic sedimentary cover of the European Platform (Karnkowski, 1974; Oszczypko, 1998, 2006).

According to Pescatore & Ślączka (1984), Roca *et al*. (1995) and Behrmann *et al*. (2000), the Outer Carpathian accretionary wedge formed in the direction from hinterland to foreland and its accretion started from the Magura nappe during the Oligocene. However, the results of synsedimentary deformation studies in the Eocene rocks of the Magura nappe suggest that the tectonic shortening started earlier during the Late Eocene (Świerczewska & Tokarski 1998). Balanced cross-section analyses have supported the earlier date (Nemčok *et al.* 2006).

The tectonic evolution of the Polish segment of the northern Outer Carpathians is characterized by the superposition of two tectonic shortening events that were connected with regional tectonic transport directed first NNW–(N) and then NE (Aleksandrowski, 1985, 1989; Decker *et al.* 1997, 1999; Zuchiewicz *et al.* 2002; Tokarski *et al.* 2006). The tectonic map of the Polish Outer Carpathians by Jankowski (2007) clearly shows the superposition of two generations of the map-scale thrusts.

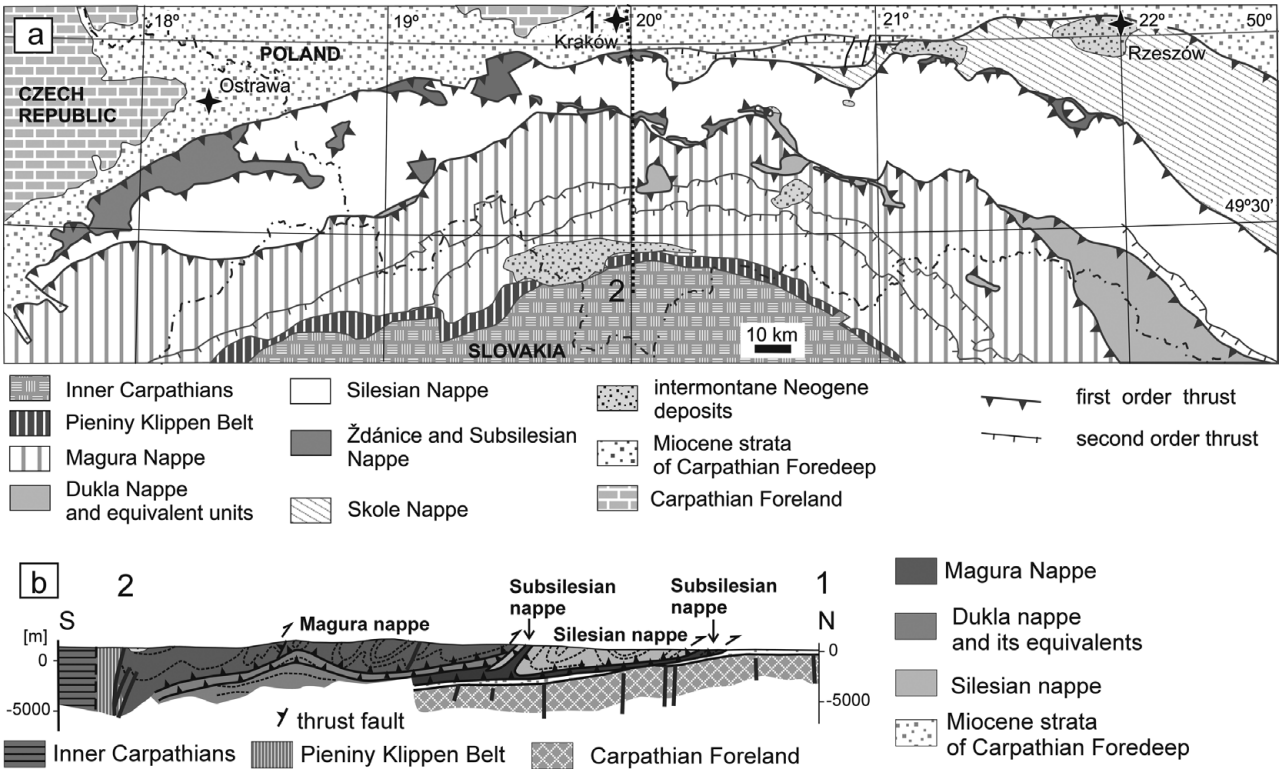

Figure 2. (a) Geological map of the Outer Carpathians modelled in this study with location of cross-section 1–2 (simplified after Żytko *et al.* 1989; Połtowicz 1991; Jankowski, 2007). (b) Simplified cross-section along line 1–2 after Żytko *et al*. (1989).

According to Aleksandrowski (1989) and Nemčok *et al*. (2007), the reconstructed σ_1 stress axis trajectories for the Magura and Silesian nappes based on the regional folds and thrusts are characterized by an overall fan-shaped pattern, which supports an earlier study of jointing in the Silesian nappe (Mastella & Konon, 2002). According to Aleksandrowski (1989) and Decker *et al*. (1999) these regional structures were formed during the first event. The first structures were then partly refolded and overprinted by the set of structures derived from the second horizontal compression oriented NE–SW (Aleksandrowski, 1989; Decker *et al.* 1997). Some NE-striking thrusts from the first shortening event were reactivated as sinistral strike-slip faults in the Polish western part of the Silesian and Magura nappes (Decker *et al.* 1997) and also further to the SW in the Czech part of the Outer Carpathians (Fodor, 1995). However, only the folds and thrusts related to the horizontal compression oriented NE–SW occur in the eastern part of the Silesian nappe (Decker *et al.* 1999; Rubinkiewicz, 2000).

The occurrence of two tectonic shortening events in the Polish Outer Carpathians connected with a *c.* 45° clockwise rotation of the regional horizontal compression has been interpreted as either due to a clockwise far-field stress rotation (Aleksandrowski, 1989; Decker *et al.* 1999) or a counter-clockwise body rotation of the Outer Carpathians (Zuchiewicz *et al.* 2002; Tokarski *et al.* 2006; Márton *et al.* 2009).

Palaeomagnetic investigations in the Western Outer Carpathians were performed mainly in the westernmost part of the belt, on rocks from the Magura and Silesian nappes (Korab *et al.* 1981; Krs *et al.* 1996; Grabowski *et al.* 2006). The Cretaceous and Palaeogene rocks of the western part of Western Outer Carpathians showed a 40°–73° counter-clockwise rotation (Korab *et al.* 1981; Krs *et al.* 1982, 1991, 1993 and 1996). Lower Cretaceous teschenitic rocks from the Silesian nappe showed an anticlockwise rotation of *c.* 14–70° (Grabowski *et al.* 2006). Further, the Eocene rocks of the Dukla nappe in the eastern part of Slovakia (Eastern Outer Carpathians) indicated a counter-clockwise rotation of *c.* 20° (Krs *et al.* 1996).

The recent systematic palaeomagnetic investigations of the Late Eocene – Oligocene strata of the Magura nappe and the Oligocene strata of the Silesian nappe in the Czech and Polish segment of the Western Outer Carpathian belt enable the post-Eocene amount of rock rotation to be recognized within the Western Outer Carpathian belt (Márton *et al.* 2009). The Magura nappe strata were rotated counter-clockwise by *c.* 50°, and these strata acquired their palaeomagnetic signals after folding. The central and eastern part of the Silesian nappe also underwent large counter-clockwise rotations (*c.* 45°) after the acquisition of the palaeomagnetic signals. The rocks of the western part of the Silesian nappe underwent a larger counter-clockwise rotation of *c.* 75°. According to Márton *et al*. (2009), such large rotations were caused by left-lateral shear related to a left-lateral wrench corridor, as documented from the Czech part of Outer Carpathians (Fodor, 1995). Márton *et al*. (2009) suggested that the

https://doi.org/10.1017/S0016756813000320 Published online by Cambridge University Press

Magura and Silesian nappes moved together after the Oligocene and that the movement was accompanied by a *c.* 50° counter-clockwise rotation.

3. Analogue modelling

Analogue modelling is a useful research method by which to understand the deformation mechanisms of individual structures or of entire orogens. The relationship between a particular structure and the experimental conditions under which it formed can therefore be better correlated. In this way, analogue modelling allows different geodynamic hypotheses to be tested for real geological structures, such as the development of fold-and-thrust belts and accretionary prisms (e.g. Davis *et al.* 1983; Mulugeta & Koyi, 1987; Davy & Cobbold, 1988; Mulugeta 1988; Zweigel, 1998; Marshak 2004; Reiter *et al.* 2011). Such analogue modelling mostly uses an indenter, which may be either a rigid block (e.g. Zweigel, 1998) or a vertical plate (e.g. Mulugeta & Koyi, 1987), to push the soft experimental material in whatever way is required.

The experimental material itself must fulfil certain rheological criteria: these materials should behave in a mechanically similar way to the brittle rocks of the upper crust and follow the Coulomb yield criterion (e.g. Mulugeta, 1988). Traditionally, dry granular materials such as sand have been used in the analogue models of tectonic processes (e.g. Hubbert, 1951; Schellart, 2000). However, the properties of wet clay are also appropriate because this ensures a dynamic similarity between the model and nature (e.g. Hubbert, 1937). In the past, analogue models have used wet clay, plasticine, silicon or mixtures of different materials (e.g. Tapponnier *et al.* 1982; Eisenstadt & Sims, 2005; Boutelier *et al.* 2008). A significant feature of dry sand is its very low cohesion (e.g. Schellart, 2000; Mechelen, 2004), with any cohesive strength being mainly due to interlocking between grains (e.g. Mechelen, 2004). The strength of dry sand can be increased through the addition of a small amount of liquid (Mechelen, 2004). Nevertheless, the low cohesion of dry sand precludes any significant folding (Eisenstadt & Sims, 2005) and any strain is essentially accommodated by faulting. Additionally, dry sand models and wet clay models produce very different results in inversion experiments: almost all faults are reactivated in the wet clay models but only a few, if any, are significantly reactivated in sand-only models (Eisenstadt & Sims, 2005). This property of wet clay meant that wet material with clay was chosen as the experimental material in the present modelling. The possibility of the reactivation of the thrust surface of already-existing nappes during experiments was a significant property of the experimental material in the present models. The results of mesostructural investigations performed by Decker *et al.* (1997) suggest that, in the western part of the Polish Outer Carpathians, the main thrust of the Magura and Fore-Magura nappes were reactivated as low-angle strike-slip faults.

The results of the indentation experiments depend on the different parameters being tested such as basal friction, the effect of sedimentary thickness, the dip of the indenter and its geometry/shape and any other factors (e.g. Colletta *et al.* 1991; Liu *et al.* 1992; Zweigel, 1998; Lickorish *et al.* 2002). In many experiments, the indenter is usually simply moved along a straight line (e.g. Zweigel, 1998). Only rarely have indenters been moved along a more complicated path such as a curve, or with an added simultaneous rotation component (e.g. Lickorish *et al.* 2002).

In indentation analogue modelling, the most popular type of indenter has been the simple vertical plate which produces frontal indentation normal to the indenter margin (e.g. Mulugeta & Koyi, 1987, 1992). Oblique indentation can be modelled when the indenter movement is not perpendicular to the frontal margin of the indenter itself, or when the shape of the indenter is curved (e.g. Zweigel, 1998; Lickorish *et al.* 2002). There have been experiments where the width of the indenter is smaller than the width of the experimental box, which produces deformation of the experimental material at the lateral indenter margins (e.g. Zweigel, 1998). Such narrower indenters were used in the experiments presented in this paper.

4. Experimental procedure

4.a. Experimental material

Unconsolidated sediment from a very small lake in the vicinity of Kolbuszowa, Poland was used for the analogue models. The lake is in an area covered by Quaternary glacial sediments, mostly sand, silt or loess. The sediment used in the models is light-grey in colour and is unstratified. Binocular microscope observations showed that, by applying Powder's Roundness Scale (Powders, 1953), the coarse silt and very fine sand are subangular to subrounded, and the fine and medium sand are rounded to well-rounded. The surfaces of sand have a frosted appearance suggestive of an aeolian origin. Zingg's shape classification (Pettijohn, 1975) would term the very fine silt as being mostly prolate, while sand is mostly equiaxial; muscovite is the exception, being triaxial.

The material used for the modelling contains *c.* 12.3% clay minerals (muscovite, smectite and illite), 7.8% albite, 8.5% microcline and the remaining 71.4% being quartz. These mineral proportions were quantified by X-ray powder diffraction. With respect to the grain size, the sediment as a whole can be classed as a sandy silt (Head, 1992), but the detailed size fractions (in weight %) are as follows: clay fraction (<0.002 mm) 6%; silt fraction (0.050–0.002 mm) 49% and sand fraction (2.00–0.05 mm) 45%.

The material has low cohesion (14.16 kPa) and small angle of internal friction of 12.12° (Table 1). The plastic limit of the material is 17.50% by weight, its liquid limit is 25.65% by weight, its plasticity index is 8.15% and its flow index is 0.21. The sandy silt used in the

https://doi.org/10.1017/S0016756813000320 Published online by Cambridge University Press

Table 1. Quantity nature model scaling ratio (model/nature)

Parameter	Nature	Model	Ratio (Model/Nature)
Density (kg m^{-3})	*c.* 2640[a]	1860	*c.* 0.7
Angle of internal friction (°)	23–32[b,c]	12.12	0.4–0.5
Cohesion (kPa)	30–6500[b,c]	14.16	0.002–0.5
Length (m)	100 000	1	1×10^{-6}
Gravity (m s^{-2})	9.81	9.81	1

[a]Average density after Stefaniuk *et al.* (2009); [b]Properties of shales after Broniatowska (2008); [c]Properties of sandstones after Łukaszewski (2007).

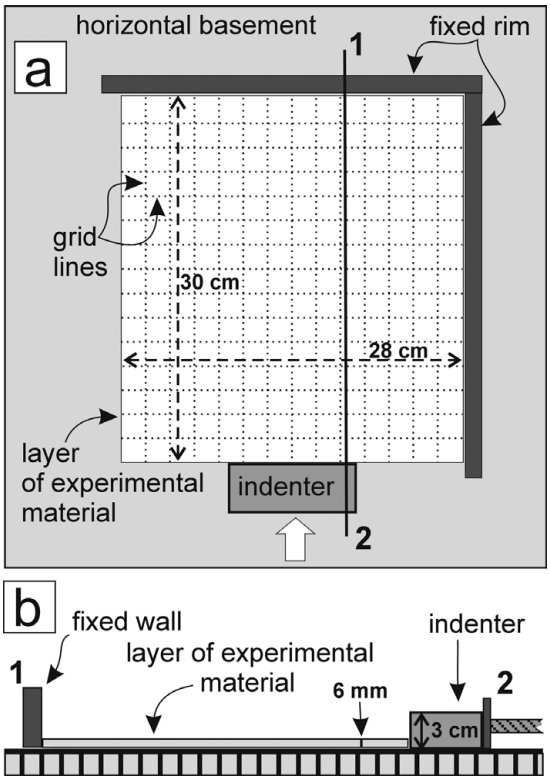

Figure 3. Diagram of the experimental apparatus. (a) Plan view of the deformation table showing analogue model start position and the rectangular indenter that was used in experiment 1 (white arrow shows the compression direction). (b) Cross-section of the deformation table with compression direction from right to left.

experiments was wet and had a density of *c.* 1.86 g cm^{-3} and a water content of *c.* 20%. A suitable water content was determined by repeated testing, because the wet sandy silt should be able to undergo brittle deformation (faulting) as well as folding. Before each experiment the sandy silt was mixed with water to form a homogeneous composition.

4.b. Model construction

All experiments were performed at the Laboratory of Analogue Modelling in the Institute of Geological Sciences, Polish Academy of Sciences. The layer of the sandy silt used in the modelling was *c.* 6 mm thick (Fig. 3). The maximum thickness of the sedimentary sequences of the Carpathian basin reached 5000 m, locally even 7000 m in the Silesian nappe (Poprawa *et al.* 2002). The vertical scaling of the model was *c.* 10^{-6}, i.e. 1 mm in the model represents 1000 m in nature. The average density of the rocks in the Polish Outer Carpathians is 2.64 g cm^{-3} (Stefaniuk *et al.* 2009).

An orthogonal grid with the mesh size of *c.* 2 × 2 cm was inscribed on top of the experimental layer. The grid enabled continuous monitoring of the deformation and rotation of the material during the experiment. Each experiment was systematically photographed. Each layer of experimental material was laid horizontally and was blocked on two sides in the direction of indentation (to the north and east) to simulate resistance by the Carpathian Foreland.

Each indenter was wooden, 3 cm thick and had vertical sides because the southern margin of the Polish Outer Carpathians is vertical or subvertical on published cross-sections (Fig. 2b). Two kinds of indenter shape were tested: a rectangular and a quasi-triangular indenter. The quasi-triangular shape resembled the present-day southern boundary of the northern Outer Carpathians (Fig. 1). The rectangular indenter was included as a typical shape of the indenter.

The base of the indenter was in contact with the table and was displaced at a constant velocity of 0.1 mm s^{-1} (36 cm h^{-1}). This indentation velocity produced thrusts that dipped towards the indenter, which were successively formed in the foreland direction. Slower indentation caused a topographic accumulation of material in front of the indenter, but without any macroscopically visible brittle deformation (e.g. thrusts). The experiments were repeated several times and revealed similar results in all cases. The length scaling of the model was 10^{-6}, i.e. 1 cm in the model represents 10 km in nature (Table 1).

4.c. Three model scenarios

Three experiments were performed, one with the rectangular indenter and two with the quasi-triangular indenter. The rectangular indenter was pushed into the sandy silt normal to its frontal margin (Fig. 3). This simple experiment was also performed for comparative purposes for the more complex quasi-triangular indenter experiments.

Reconstructions of the Oligocene–Miocene tectonic evolution of the Pannonian–Carpathian system (e.g. Kováč *et al.* 1994; Fodor *et al.* 1999; Nemčok *et al.* 1998*a*) suggest that the ALCAPA block moved north- and eastwards with a probable simultaneous counter-clockwise rotation during the Miocene. Additionally, detailed mesostructural research on the Western Outer Carpathians (Aleksandrowski, 1989; Decker *et al.* 1997, 1999; Tokarski *et al.* 2006) suggests that there were two different directions of the regional tectonic transport caused by the motion of the hinterland/ALCAPA block, both of which were oriented first N–S and then NE–SW. In the laboratory, the different ways that the indenter/ALCAPA block movement were tested. The experimental procedures differentiated

https://doi.org/10.1017/S0016756813000320 Published online by Cambridge University Press

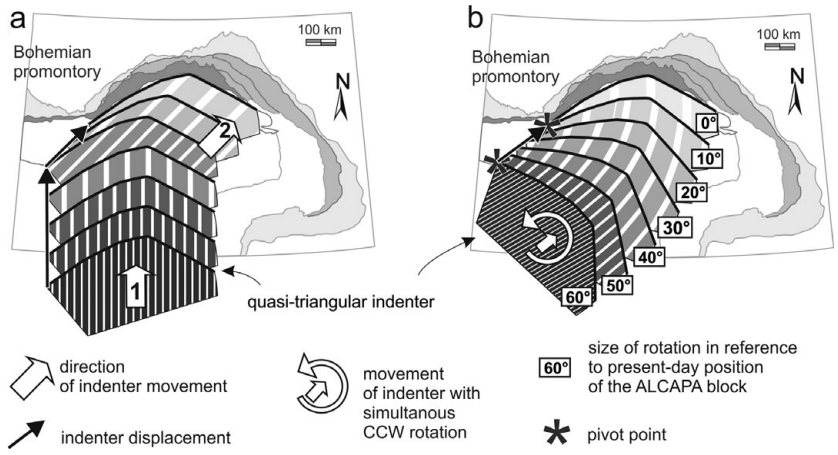

Figure 4. Schematic scenarios of experiments 2 and 3, which used a quasi-triangular indenter. (a) Experiment 2, in which the indenter was pushed initially to the north (in present geographic coordinates) and then to the NE. (b) Experiment 3, in which the indenter was pushed ENE but with a simultaneous anticlockwise rotation of *c.* 60°. The quasi-triangular shape of the indenter was intended to resemble the present-day southern boundary of the northern Outer Carpathians. Geological map of the Carpathian–Pannonian–Dinaride region after Csontos *et al*. (1992).

between the direction of indenter movement and the presence of a simultaneous anticlockwise rotation. The two types of experiments (Fig. 4a, b) were: (1) the quasi-triangular indenter was pushed in two successive directions that varied by *c.* 45°, i.e. the indenter was pushed first to the north (in relation to present geographic coordinates) and then to the northeast; and (2) the quasi-triangular indenter was pushed in one defined direction (NE–SW in relation to present geographic coordinates) with a simultaneous counter-clockwise rotation of *c.* 60°. The amount of indenter rotation was determined on the basis of palaeomagnetic investigations of the Oligocene Podhale Flysch (Inner Western Carpathians, south of the Pieniny Klippen Belt), which suggested that this flysch underwent an anticlockwise rotation of *c.* 60° (Márton *et al.* 1999).

The amount of Oligocene–Miocene displacement of the ALCAPA block has also been much debated. Shortening of the western part of the northern Outer Carpathians along a NW–SE profile reached a maximum of 160 km (Picha *et al.* 2005); the shortening of the eastern part of the northern Outer Carpathians along a NE–SW profile reached a maximum of 260 km (e.g. Behrmann *et al.* 2000). The amount of the continental escape of the ALCAPA block is estimated as 60–100 km in the Alps (Schmid *et al.* 1989).

The type of experimental material used imposed the additional difficulty of selecting the length of indentation. According to Eisenstadt & Sims (2005), indenter movement at the start of an analogue experiment into wet clay (and wet sandy silt) does not cause the formation of macroscopically visible overthrusts. In the present experiments, the displacement size of the indenter was therefore chosen arbitrarily and was dependent on the suitable quantity of slices in experimental prism, the equivalents of nappes in the real Carpathian belt. In consideration of that fact, the displacement size of the indenter was greater than suggested in the literature. Conversion of the distance in the model to the distance in the Carpathian area shows that the amount of the indenter displacement reached *c.* 450 km in the first experiment with the rectangular indenter, 600 km (400 km to the north, 200 km to the northeast) in the second experiment with the quasi-triangular indenter and 210 km (in reference to the rotation pivot of indenter) in the third experiment (Fig. 4).

Corner effects at the Bohemian promontory have also been considered an important factor which influence the style of ALCAPA block movement during its Neogene emplacement into the Carpathian embayment (Sperner *et al.* 2002; Ratschbacher *et al.* 1991*b*; Bada, 1999). In the experiment with the rotation of the quasi-triangular indenter, the position of the pole of rotation was therefore the position associated with and assumed for the Bohemian Massif (Fig. 4b).

5. Experimental results for the three scenarios

5.a. Experiment 1: model with rectangular indenter

5.a.1. Experiment 1 results

In this experiment the indenter was 12 cm wide and had a rectangular shape. The experimental layer was 30 cm long and 28 cm wide (Fig. 5a). The indenter was pushed into the wet sandy silt perpendicular to its leading edge and parallel to its lateral edges.

The forward motion of the indenter deformed the experimental layer such that the grid lines became curved and there was a simultaneous lateral and horizontal escape of experimental material. This lateral escape manifested as lateral bending of the experimental layer. The left (referred to below as western) side of the sandy silt layer was not blocked, so the bending was more strongly developed on that side. The originally orthogonal grid lines (Fig. 5a) became non-orthogonal in the deformed region in front of the moving indenter (Fig. 5b); these lines recorded a penetrative shear strain.

https://doi.org/10.1017/S0016756813000320 Published online by Cambridge University Press

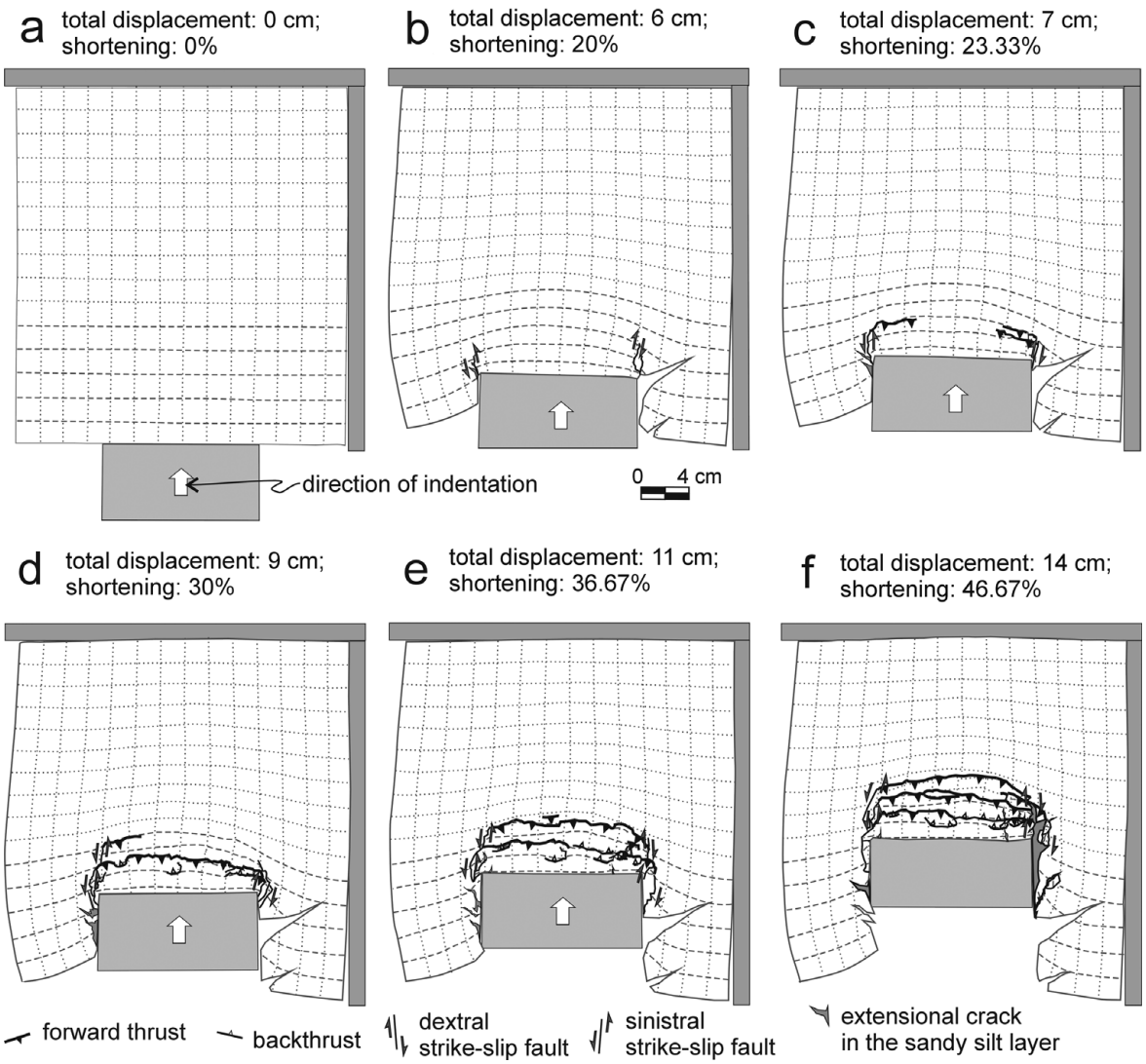

Figure 5. Line drawings taken from photographs of the model of experiment 1, which utilized a rectangular indenter. The drawings show the deformation style during the chosen stages of Experiment 1.

In relation to the middle of the indenter, the longitudinal grid lines rotated clockwise in front of the left-hand (western) side of the indenter and counter-clockwise on the right-hand (eastern) side. At the same time the latitudinal lines rotated counter-clockwise on the left-hand (western) side of the indenter and clockwise on the right-hand (eastern) side. The majority of grid meshes in the deformed part of the experimental layer in front of the prism were therefore rhomboid in shape, indicative of simple shearing, a feature also visible on both sides of the frontal part of prism (Fig. 5f). Whereas the rear part of the prism underwent pure shearing, as indicated by the style of grid line deformation, the grids have been squeezed perpendicular to the frontal indenter margin and stretched parallel to it (Fig. 5b). Grid lines were deformed well beyond the range of the prism: after only 20% shortening, nearly all the grid lines were deformed except for the last one in the most distal part of the experimental layer (Fig. 5b). All grid lines were deformed after 23.33% shortening. Such deformation of the grid lines suggested a long distance of penetration of the stress in the wet sandy silt layer without any significant faults except the basal detachment of this experimental layer from the basement.

At about 20% shortening of the model (Fig. 5b) the material was accumulated as the topographical elevation at the front of the moving indenter, but there was no sign of macroscopically visible brittle deformation within such a wedge. This wedge, called a protoprism, was laterally terminated by steeply dipping transfer faults (Fig. 6). These transfer faults had the character of tear faults, and they were formed in the indenter lateral edge prolongation and penetrated the whole layer of experimental material. The indenter lateral edges were parallel to the direction of indentation.

Main thrusts were initiated as segments (Fig. 5c) and these smaller thrusts propagated laterally and, with increasing indenter displacement, became linked together across the model by the transfer faults mostly in the form of oblique thrusts (Fig. 5d). Each trace of the main thrust was therefore not linear but varied

https://doi.org/10.1017/S0016756813000320 Published online by Cambridge University Press

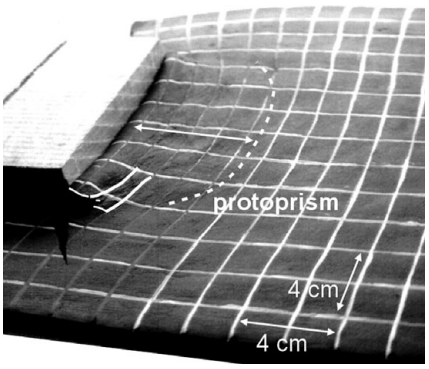

Figure 6. Photograph showing an oblique view of the model of experiment 1 (rectangular indenter displacement is 7 cm; bulk shortening is 23.33%).

along-strike. At the beginning, the trace of almost every new small thrust at the front of the prism was slightly arched. The lateral linking of such thrusts was finished by formation of the large thrust whose trace was also in general arched (Fig. 5d). Further indentation forced the prism to grow and caused a straightening of the traces of older, inner thrusts so that these became nearly parallel to the frontal margin of the rectangular indenter (compare Figs 5d–f).

Main thrusts were formed in the sequence towards the indenter's foreland and dipped towards the indenter. There were also a small number of thrusts that dipped in opposite directions and accompanied the main thrusts, interpreted as back-thrusts (Fig. 5e).

The markers in the rear part of the prism (Fig. 7, a–g markers) showed that, at the start of the experiment, the innermost slice bent convexly to the foreland when there was up to 23.33% shortening (Figs 5c, 7a). Further indentation caused a straightening of this slice (Figs 5e, 7) and, later, its bending in the opposite direction (convexly to the hinterland). This latter geometry resulted from back-thrusting of the experimental prism over the indenter (Figs 5f, 7). The markers in front of the prism (Fig. 7; h–p markers) showed continuous bending of the material convexly to the foreland during the whole experiment (Fig. 7b).

5.a.2. Experiment 1: comparison between the model and the Western Outer Carpathians

The rectangular indenter was used in the first experiment. Although the outline of the experimental prism was convex to the north (Fig. 5f), the model with the rectangular indenter did not produce a sufficiently arcuate geometry as compared to the northern Outer Carpathians (Fig. 8a). Additionally, the traces of the main thrust in the northern Outer Carpathians are curved convexly to the foreland and are not sharply terminated on transfer faults striking N–S as in model 1 (Fig. 8a).

In the eastern part of the northern Outer Carpathians (northern part of the Eastern Outer Carpathians), the traces of the main thrusts are almost straight and parallel to each other, parallel to the frontal margin of the Carpathian wedge and parallel to the southern boundary of the Carpathian wedge (Fig. 1). This type of wedge geometry could be produced by the rectangular indenter moving to the NE (azimuth of indentation direction, N 30° E). However, such a model (Fig. 5f) is abruptly terminated on tear faults at both its sides, suggesting that the correct type of indenter for simulating the evolution of the Western Carpathian wedge should be less curved on its western side compared to the right corner of the rectangular indenter (Fig. 8b). The rectangular indenter model shows neither the presence of two successive stages of tectonic shortening nor well-marked counter-clockwise horizontal rotation of rocks within the prism.

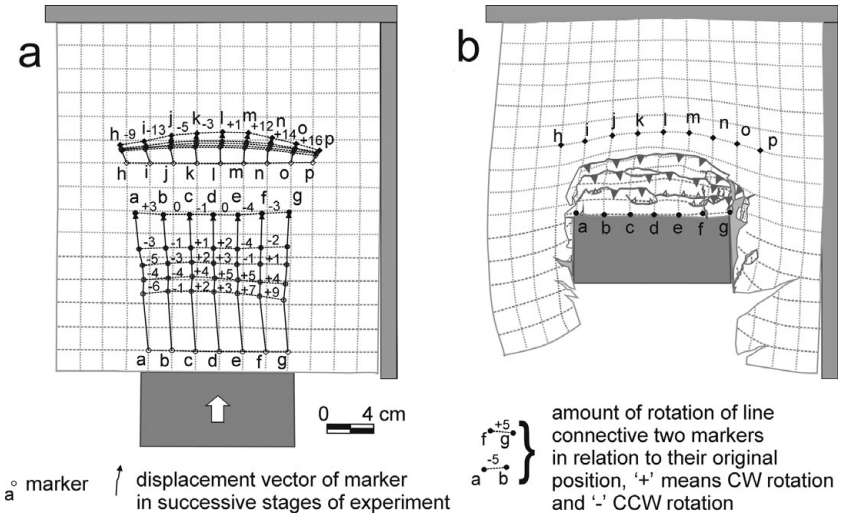

Figure 7. Marker orientations from experiment 1, which used a rectangular indenter. (a) Sketch of the original model before the experiment showing the location of markers through the whole experiment. (b) Sketch of the final model with the final orientation of the markers.

https://doi.org/10.1017/S0016756813000320 Published online by Cambridge University Press

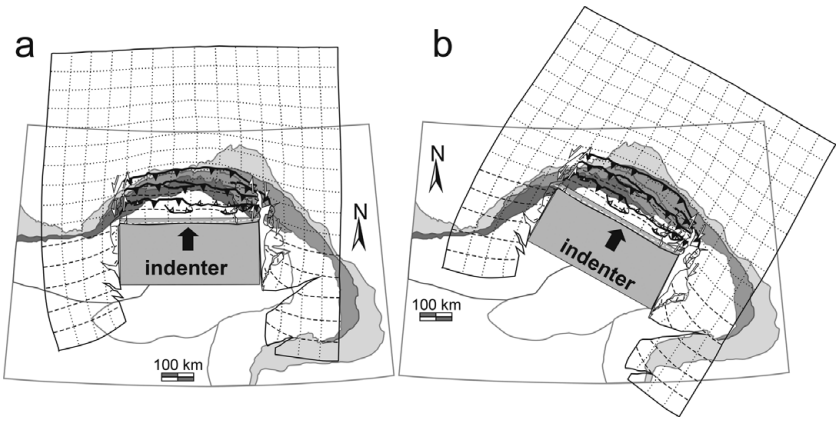

Figure 8. Comparison between model 1 (see Fig. 5f) and the map-view of the main tectonic features of the Carpathian area (after Csontos *et al.* 1992). (a) Indentation direction N 0° E. (b) Indentation direction N 30° E.

5.b. Experiment 2: model with quasi-triangular indenter moved in two successive directions

5.b.1. Experiment 2 results

In experiment 2, the experimental layer was 30 cm long and 28 cm wide, and the shape of the indenter was quasi-triangular in order to resemble the shape of the ALCAPA block (Fig. 9a). The experiment was divided into 2 stages: first, the indenter was moved northwards (relative to present geographic coordinates; Figs 9a–e); second, and subsequent to the first stage, the indenter was moved to the NE (Fig. 9f).

At the beginning of the indentation process when there was up to 14.61% shortening (Fig. 9b), the observed processes were very similar to Experiment 1: accumulation of material at the indenter front, but no sign of brittle deformation (Fig. 10); curvature of the grid lines; and lateral escape of material (Fig. 9b). The originally orthogonal grid lines (Fig. 9A) were deformed in front of the moving indenter in an opposing style relative to the apex of the quasi-triangular indenter (Fig. 9b). The longitudinal grid lines rotated counter-clockwise on the left-hand (western) side of the indenter apex and clockwise on its right-hand (eastern) side. The majority of the grid meshes in the deformed part of the experimental layer had a rhomboid shape, indicative, as for Experiment 1, of simple shearing. The grid meshes at the rear (southern) part of the experimental layer showed that this material underwent a rotation component. In this rear zone, the material deformed via pure shear: the grid meshes were squeezed perpendicular to the frontal indenter margin and were stretched parallel to this margin (Fig. 9b).

During the first northwards stage (Fig. 9a–e), the trace of a newly formed thrust was slightly arched, convex to the foreland. In the initial phase of thrust formation, the trace of its fault line disappeared laterally. The main thrusts initiated as segments of small thrusts (Fig. 9d) that laterally propagated and linked across the model with increased displacement of the faults (Fig. 9e; note thrusts in the frontal part of the experimental prism). Increased fault displacement caused the formation of transfer faults as the lateral termination of thrust propagation (Fig. 9e). On the left-hand (western) side of the indenter apex, where the experimental layer was not blocked and the indenter margin was less oblique to the indentation direction, the thrusts terminated on tear faults (Fig. 9e). On the right-hand (eastern) side of the apex, tear faults seldom occurred but oblique thrusts were formed (Fig. 9e). In relation to present geographic coordinates, the tear fault traces were orientated in three predominant ways (Fig. 9e): (1) mostly NNE–SSW in the left-hand (western) side of the experimental prism (in relation to the apex of the indenter); (2) mostly NNW–SSE (to NW–SE) and NNE–SSW in front of the indenter's apex; and (3) mostly NNE–SSW on the right-hand (eastern) side of the experimental prism.

The main thrust that developed during this experiment dipped towards the indenter. Back-thrusts only occurred in small numbers and accompanied the main faults (Fig. 9e). After the indenter was displaced by 11 cm (Fig. 9d) the traces of any new faults were almost perpendicular to the direction of indenter movement. By this time, the older/inner thrust had become more curved and slightly mimicked the indenter shape. In relation to present geographic coordinates, the thrust traces were orientated in three main ways (Fig. 9e): (1) mostly WSW–ENE (N 65–80° E), with rare W–E trends and a local SW–NE trend in the left-hand side of the experimental prism (in relation to the apex of the indenter); (2) mostly W–E in front of the indenter apex; and (3) mostly WNW–ESE (N 110–125° E) with a rare W–E trend, or a local SW–NW trend (note oblique thrust in the frontal part of the prism) in the right-hand (eastern) side of the experimental prism. The traces of the inner thrusts are strongly curved convex to the foreland, the orientation of these traces roughly mimicking the quasi-triangular outline of the indenter. The outline of the prism (the first stage of experiment 2) was nearly linear in its central part and more curved in its eastern part, where the oblique thrusts were formed. The western side of the prism was characterized by

https://doi.org/10.1017/S0016756813000320 Published online by Cambridge University Press

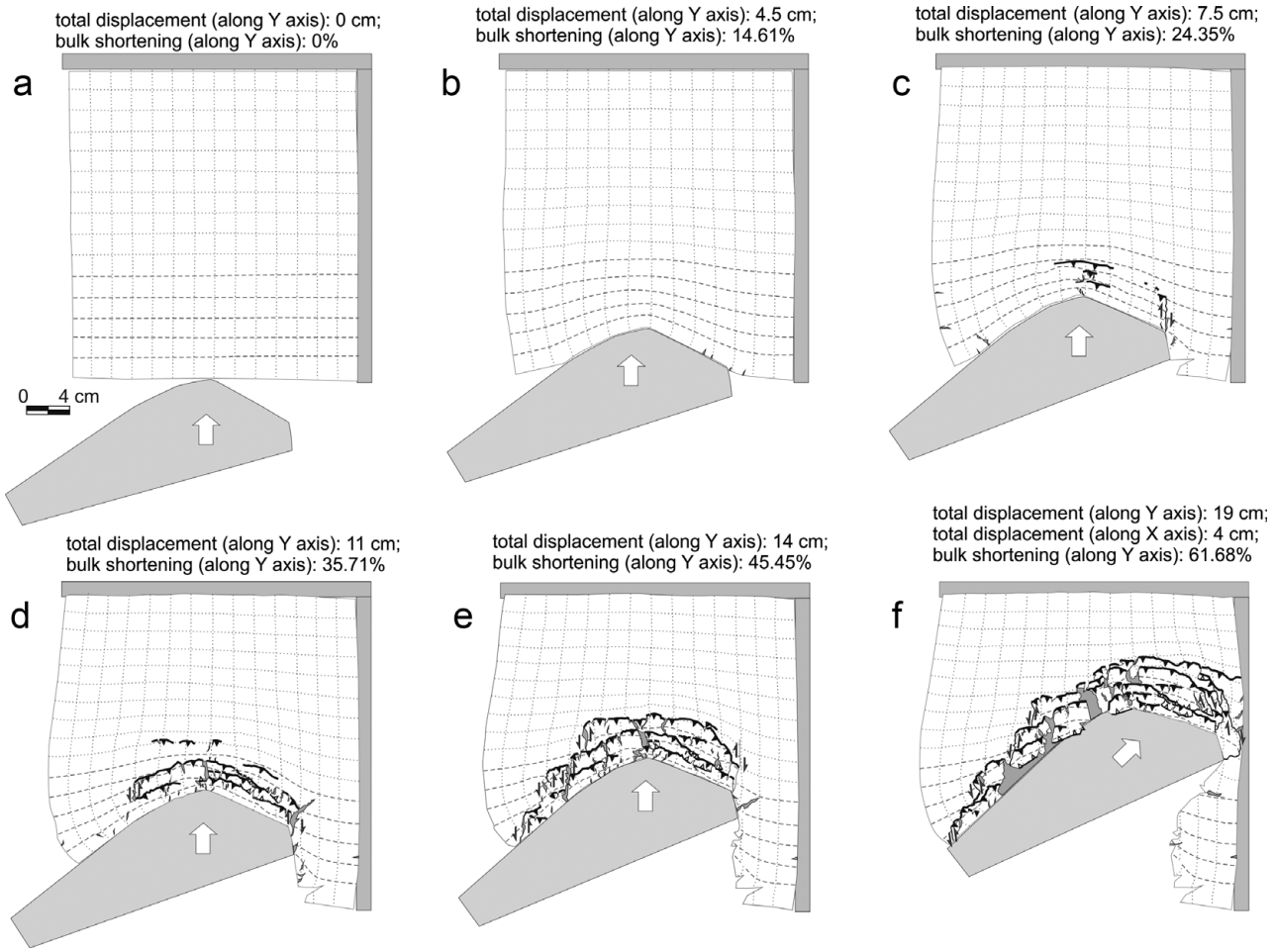

Figure 9. Line drawings taken from photographs of the model of experiment 2, which used a quasi-triangular indenter moving in the two successive directions (same legend as in Fig. 5). The drawings show the deformation style of two-stage model during both stages.

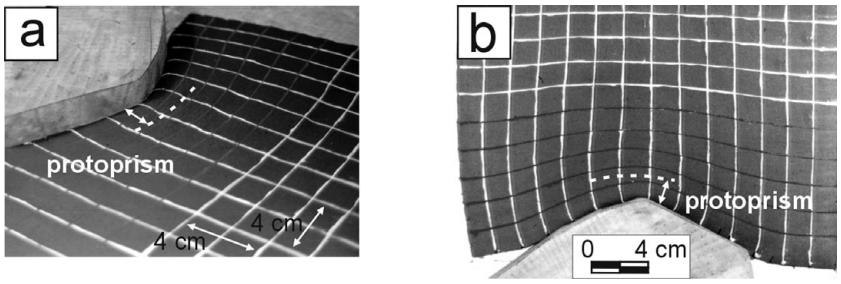

Figure 10. (a) Oblique frontal and (b) top-view of experiment 2, which used a quasi-triangular indenter after 14.61% bulk shortening; see Figure 9b for the map-view of the model.

the step-like geometry of the outline, because the main thrusts terminated westerly on a tear fault.

Numerous tension gashes formed within the whole experimental prism (Fig. 9c–e). These structures were particularly numerous in front of the left-hand (western) side of the quasi-triangular indenter which had a less oblique margin to the indentation direction compared to its eastern margin (Fig. 9e). All the observed extensional cracks were orientated predominantly NNW–SSE and N–S, with a rare subset oriented NW–SE and some locally NNE–SSW at the left-hand (western) side of the experimental wedge (Fig. 9e). At the right-hand (eastern) side of the wedge, tension cracks were less frequent and were oriented mostly NNE–SSW or N–S. This side of the model was blocked. The E–W extension exerted the largest influence at the front of the indenter apex and was marked by a formation of large gaps within the wet sand silt. The orientation of the extensional structures suggests they may be viewed as orogen-parallel extension within the experimental prism (Fig. 9e).

The second stage of the experiment was when the indenter was then moved to the NE (in relation to present geographic coordinates). During this phase, a new structure formed at the right-hand (eastern) side of the experimental prism (Fig. 9f). At the left-hand

https://doi.org/10.1017/S0016756813000320 Published online by Cambridge University Press

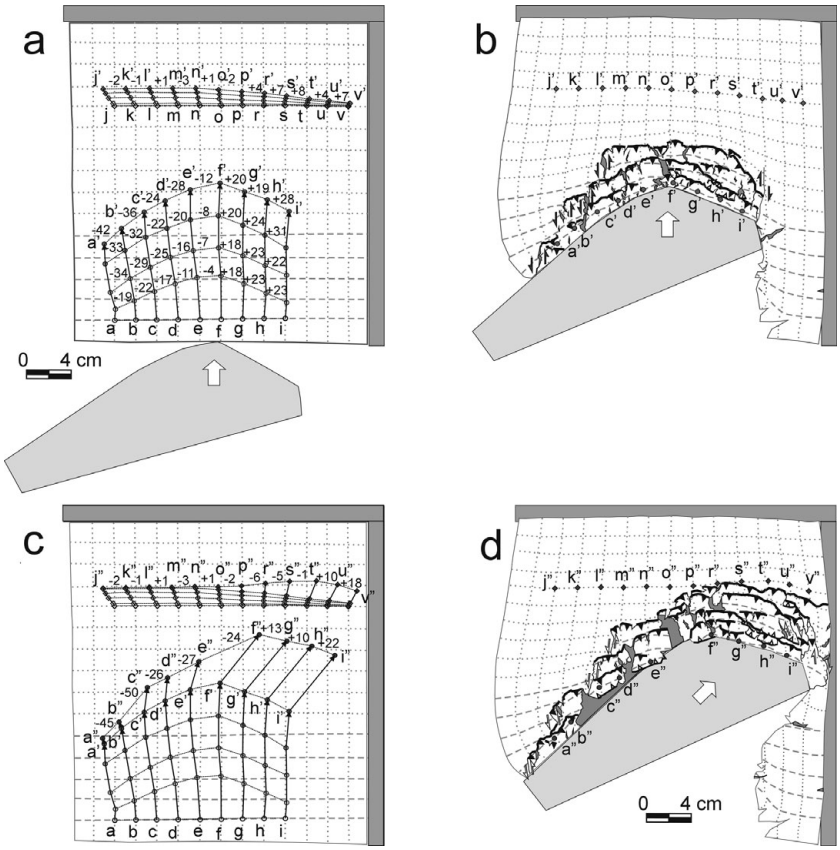

Figure 11. Marker orientations from the two-stage model of experiment 2, which used a quasi-triangular indenter. (a) Sketch of the original model before the experiment showing the location of markers through the first stage of the experiment. (b) Sketch of the final model of the first stage with the final location of the markers at this stage. (c) Sketch of the original experimental layer showing the location of markers through the whole two-stage experiment. (d) Sketch of the final location of the markers in this experiment. A letter of the alphabet was a symbol of each marker; numbers show the amount of rotation of the hypothetical line which jointed the neighbouring markers; – means anticlockwise rotation; + means clockwise rotation in comparison to the original position of markers. Other symbols as in Figure 7.

(western) side of the model, the older thrust surfaces were reactivated as sinistral faults. The numerous tension gashes formed here during the first stage became increasingly stretched. At the right-hand side of the model, the tension gashes remained weakly developed. At the left-hand side of the model at the end of the experiment, the thrust traces were oriented mostly WSW–ENE (N60–80°E), locally SW–NE or even NNE–SSW in the southern-most part of the model, and E–W in its northern part. At the end of the experiment, the thrust traces were oriented mostly W–E and WNW–ESE (N 110–120° E) and locally NW–SE at the eastern part of the model. Also at the eastern part, the older slices which had formed during the first event were slightly counter-clockwise rotated by up to 5–10°, as determined from the rotation of the longitudinal grid lines and the previous orientation of the thrusts (Fig. 11). In the western part of the model, the older slices were also locally rotated by *c.* 5–10° either clockwise (Fig. 9f, see slice partly back-thrusted over the indenter) or counter-clockwise (Fig. 9f, see the most northern slice). The slices in the experimental wedge also underwent simple shearing (Fig. 9f; see the rhomboid shape of the originally rectangular grid meshes). The real rotation of the experimental material should therefore be slightly different from the rotation determined via orientation of the longitudinal grid lines (Fig. 11). Back-thrusts were observed mostly in the rear part of the model, but also locally in the central part where single small slices were back-thrusted over the indenter.

5.b.2. Experiment 2: a comparison between model 2 and the Outer Carpathians

The first stage of experiment 2 with indentation northwards produced a roughly symmetrical final model, omitting the lateral termination of the main thrusts. The thrust traces of the inner slices of the experimental wedge were oriented roughly similar to the outline of the indenter.

In the model the main thrusts were sharply terminated laterally and westwards on sinistral tear faults. In the western part of the Western Outer Carpathians, the main thrusts of the Magura and Silesian nappes were not laterally or sharply terminated on tear faults (Fig. 12a). Nevertheless, the trace of the frontal thrust of the Magura nappe shows a stair-like outline, which may suggest that the Magura nappe could have been formed during such oriented indentation. The first

https://doi.org/10.1017/S0016756813000320 Published online by Cambridge University Press

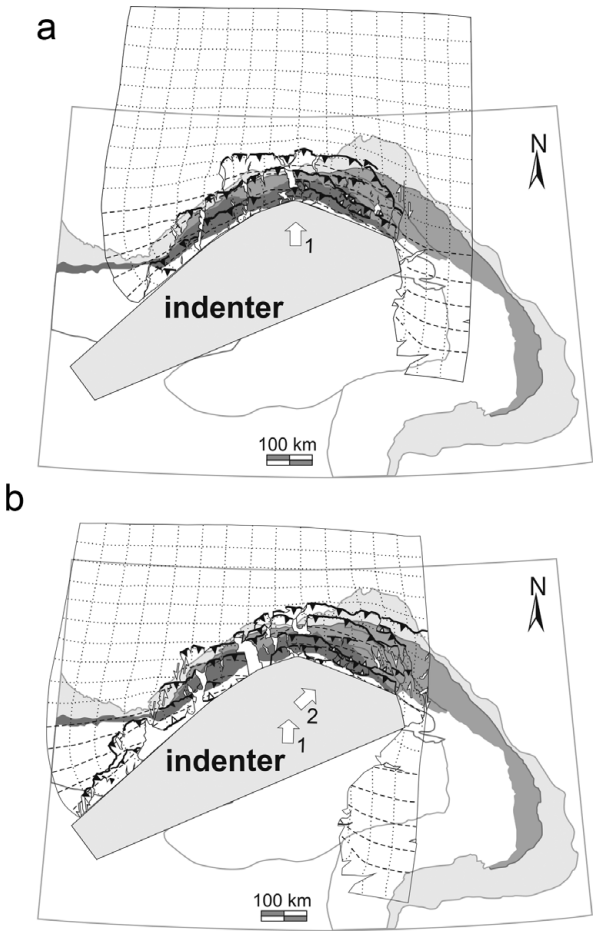

Figure 12. Comparison between the results of the two-stage model of experiment 2, which used a quasi-triangular indenter moving in two successive directions (Fig. 9) and the map-view of the Carpathian area (after Csontos *et al.* 1992). (a) End of the first stage of the experiment after indentation to N (Fig. 9e) and (b) final stage (Fig. 9f).

stage of experiment 2 explains the presence of the tectonic shortening which is related to the horizontal N–S compression, but not NE-SW compression. The occurrence of the second shortening event may be explainable in terms of stage 2 of this experiment.

Stage 2 of the model with the quasi-triangular indenter produces a more curved geometry, more compatible with that of the Western Outer Carpathians than that produced only by stage 1 (Fig. 12). A map-view geometry of the model corresponds to the geometry of the inner part of the northern Outer Carpathians, i.e. it seems to model the Magura nappe (Fig. 12a). Today, the trace of the frontal thrust of the Magura nappe in the western part of the Western Outer Carpathians has a stair-like outline (Fig. 2a; see also Żytko *et al.* 1989 and Lexa *et al.* 2000). Comparison between the two-stage model of the second experiment and the real Outer Carpathians (Fig. 12a) suggests that the innermost part of the northern Outer Carpathians could have been formed as a result of northwards indentation by the ALCAPA block, in relation to the present-day position of the ALCAPA block and Outer Carpathians. The two-stage model explains the occurrence of the two shortening events in the Western Outer Carpathians as a result of change of movement direction of the ALCAPA block.

However, there are large differences between the model and the real orogen. In the western part of the two-stage model, the sharp lateral termination of the main thrusts on the tear faults were still visible. In the western part of the Western Outer Carpathians, the main thrusts of the Magura and Silesian nappes were not so sharply terminated on tear faults as in the model (Fig. 12). Additionally, the counter-clockwise rotation of the rocks was detected along most of the northern Outer Carpathians while the experimental material rotated counter-clockwise in the western part of the prism (related to the western part of the northern Outer Carpathians) and clockwise in its eastern part (Fig. 11).

5.c. Experiment 3: model with quasi-triangular indenter rotated and simultaneously moved in one direction

5.c.1. Experiment 3 results

For experiment 3, the width of the experimental layer was 26 cm and the lengths of the layer sides were 26 and 35 cm (Fig. 13a). The shape of the indenter was also quasi-triangular in this experiment, resembling the shape of the ALCAPA block (Fig. 4b). The model simulated movement of the ALCAPA block in the NE direction (in relation to present-day geographic coordinates) but with a simultaneous counter-clockwise rotation of *c.* 60°. This rotation was constant throughout the whole experiment, the indenter moved to the NE, and the rotation axis was located at the western end of the indenter (Figs 4b, 13).

The progressive indentation caused the grid lines to curve in front of the moving indenter, as in Experiments 1 and 2 (Fig. 13b). During the whole of Experiment 3, the zone of curvature of the grid lines was also visible in front of the experimental prism (Fig. 13b–g). However, the penetration range of the shear strain was here significantly smaller than for the other two experiments (compare Figs 5, 9, 13). The shear strain which showed up as lateral bending of the experimental layer in the previous experiments was not visible in this model (Fig. 13g). Latitudinal grid lines were rotated counter-clockwise in front of the western part of the indenter and clockwise in front of its eastern part (Fig. 13c). Longitudinal grid lines were rotated counter-clockwise almost in front of the entire indenter. The slices of the western part of the prism rotated counter-clockwise. The degree of primary counter-clockwise rotation of the slices was increased by the additional counter-clockwise rotation of the prism together with the indenter. The degree of primary clockwise rotation of the slices in the eastern part of the experimental prism was reduced by progressive counter-clockwise rotation of the whole prism together with the indenter (Fig. 13g).

https://doi.org/10.1017/S0016756813000320 Published online by Cambridge University Press

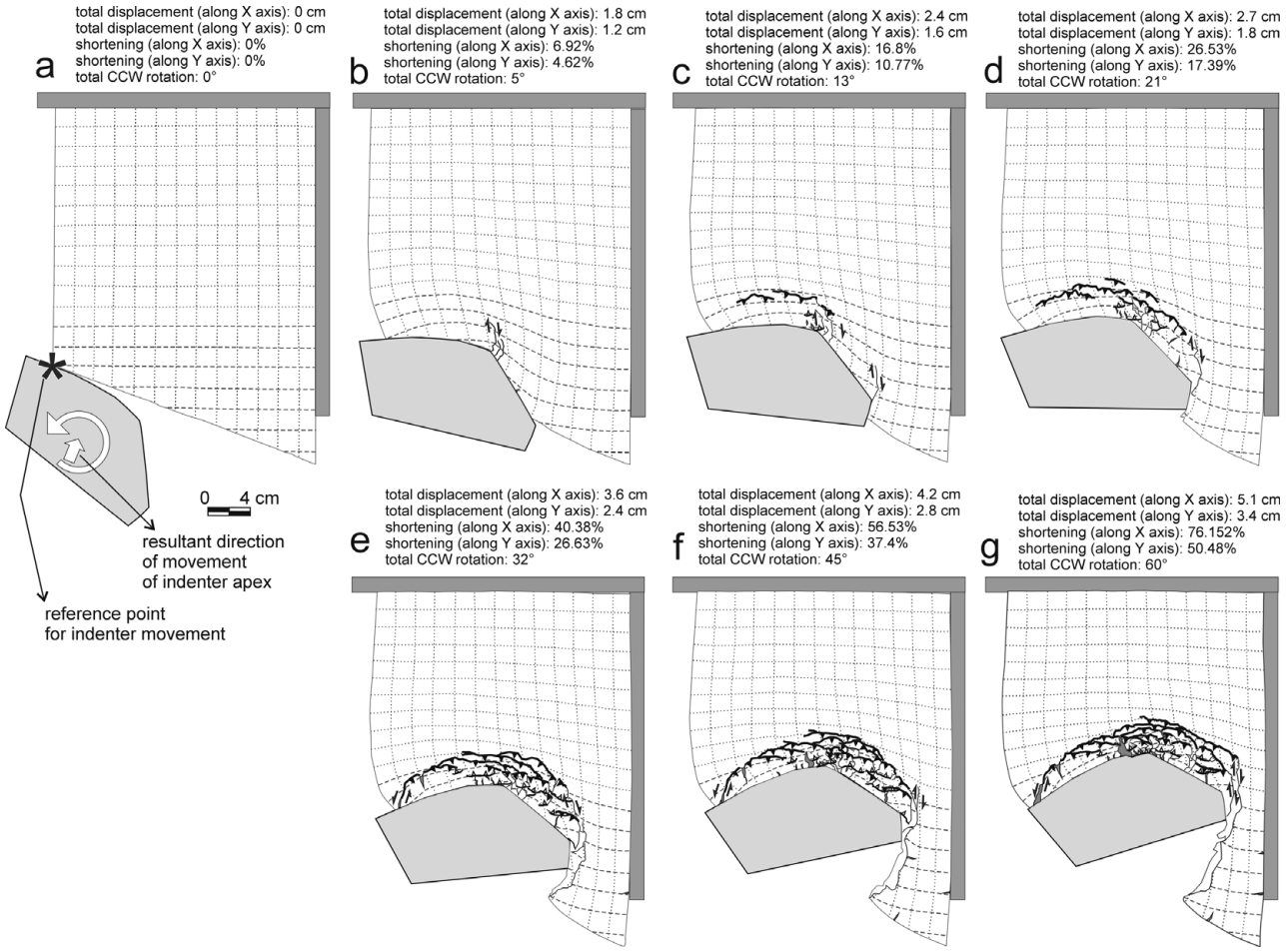

Figure 13. Line drawings from photographs of model of experiment 3. In this experiment the quasi-triangular indenter moved to the NE and simultaneously rotated anticlockwise (same legend as in Fig. 5). The drawings show the deformation style of model during the chosen stages of experiment 3.

During initial indentation (up to 6.92% shortening along the longitudinal direction), material accumulated at the front of the moving indenter and was only manifested topographically as an elevation of the material, i.e. there was no macroscopically visible brittle deformation (Fig. 13b). During this initial indentation, the left-hand (western) side margin of the quasi-rectangular indenter was roughly perpendicular to the resultant direction of the indenter apex movement and its right-hand (eastern) side margin was almost oriented at an acute angle to this direction, a simplification of reality similar to that used in experiment 1 (Figs 4a, 13a). As a result of such orientation of the indenter compared to the indentation direction, dextral tear faults formed in front of the indenter's apex as this was the sharp edge of the indenter (Fig. 13b).

Thrusts that developed as experiment 3 progressed were gently curved, convex towards the foreland and roughly perpendicular to the direction of indentation (e.g. Fig. 13c, d). In the initial phase of thrust formation, the trace of the fault line disappeared laterally. The thrusts initiated as segments (e.g. Fig. 13d; see the thrusts in the frontal part of the experimental prism) that laterally propagated and linked across the model with increased displacement on the faults (Fig. 13e). In the western part of the model, the thrusts terminated mostly as oblique thrusts (Fig. 13f); only one tear fault was formed here and this fault was located at the SW end of the experimental wedge. A different situation developed in the eastern part of the model with respect to the indenter's apex. The majority of the thrusts in this inner part of the experimental wedge laterally terminated on tear faults (e.g. Fig. 13e). Starting from a position of 26.53% shortening (along the longitudinal direction), a major thrust formed at the front of the experimental wedge and was laterally terminated eastwards as an oblique thrust (Fig. 13e). The traces of the majority of the thrusts were parallel or subparallel to the orientation of the indenter margin in the eastern part of the final model, with the exception of the oblique thrusts (Fig. 13g).

A different situation developed in the western part of the model. The outline of this part of the experimental wedge was nearly parallel to the orientation of the indenter margin. The frontal thrusts of the experimental wedge were mostly composed of the segments of the different oblique thrusts (an exception was one internal slice; Fig. 13g). The direction of the thrust traces varied significantly at the front of the indenter apex in the final model, ranging from NE–SW through W–E to NW–SE.

https://doi.org/10.1017/S0016756813000320 Published online by Cambridge University Press

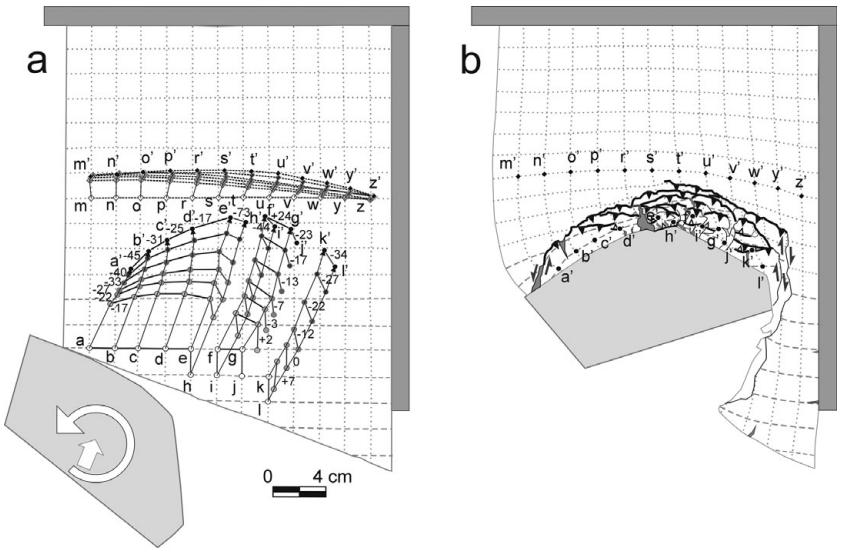

Figure 14. Marker orientations during experiment with quasi-triangular indenter moved to the NE and simultaneously rotated anticlockwise. (a) Sketch of the original model before the experiment with the orientation of markers through the whole experiment. (b) Sketch of final model with final orientation of the observed markers. Symbols as in Figures 7 and 11.

The markers in the western part of the experimental wedge (Fig. 14; a–d markers) showed that this part of the wedge curved convexly towards the foreland when shortening was up to 6.92% (compare Fig. 13b). Further indentation caused a slight straightening of this part of the slice and the simultaneous progressive counter-clockwise rotation of the prism together with the indenter (Fig. 14a). Observations of the grid mesh squares in front of the western part of the indenter showed that the grid meshes were initially deformed into rhomboid shapes (Fig. 13b) and subsequently into rectangular shapes (Fig. 13e). The grid meshes in the final model suggest that the experimental material was squeezed perpendicular to the frontal indenter margin and stretched parallel to it (Fig. 13g).

Observations of the grid mesh squares in the eastern part of the experimental wedge showed that the grid meshes underwent a large degree of simple shearing (Fig. 13g). The longitudinal grid lines were first rotated clockwise (Fig. 14a; see f–g markers) and then rotated counter-clockwise, as a result of the counter-clockwise rotation of the prism together with the indenter. The markers at the front of the prism (Fig. 14; m–z markers) showed that there was a continuous slight bending of this part of the material convexly to the foreland, and this was connected to a slight clockwise rotation of this bend (Fig. 7b).

5.c.2. Experiment 3: a comparison between model 3 and the Outer Carpathians

In the third experiment the quasi-triangular indenter was moved NE and simultaneously rotated counter-clockwise by *c.* 60°. The orientation of the trace lines of the main thrusts in the model are roughly the same as for the real Outer Carpathians, especially in the northern part of the experimental model (Fig. 2a; see also Żytko *et al.* 1989; Lexa *et al.* 2000). The thrusts in the western part of the prism terminated on sinistral oblique thrusts. A comparison between experiment 3 and the Outer Carpathians reveals that the Silesian nappe seems to fit well with the model: this nappe terminates westwards on the frontal Magura thrust and the trace of the frontal thrust of the Silesian nappe has the same oblique orientation as in the model (compare Figs 2a, 15). The innermost slice, corresponding to the Magura nappe of the Outer Carpathians, extends to the western-most end of the experimental prism as in the northern Outer Carpathians. However, the trace of the frontal thrust of this slice is only slightly convex to the north in comparison to the real orogen. Additionally, the trace of this thrust does not show the stair-like outline of the trace of the frontal thrust of the Magura nappe in the western part of the Western Outer Carpathians (Fig. 2a).

The eastern part of the model shows structures that correlate with those seen in the northern Outer Carpathians (Fig. 1). Namely, the traces of the thrusts in the model are parallel to each other and parallel to the orientation of the eastern margin of the indenter (Fig. 15). The counter-clockwise rotation of the experimental material in the western and central parts of the prism is quite well recorded in experiment 3 (Fig. 14). These parts of the experimental prism correspond to the Western Outer Carpathians (Fig. 15).

The map-view geometry of model 3 roughly corresponds to the geometry of the northern Outer Carpathians (Fig. 15). The outline of this experimental prism is appropriately arcuate when compared to the northern Outer Carpathians; it is asymmetrical and is wider in its eastern part. This experiment explains the occurrence of two shortening events and the counter-clockwise rotation of rocks within the Western Outer Carpathians. The northern Outer Carpathians could therefore be formed in front of the

https://doi.org/10.1017/S0016756813000320 Published online by Cambridge University Press

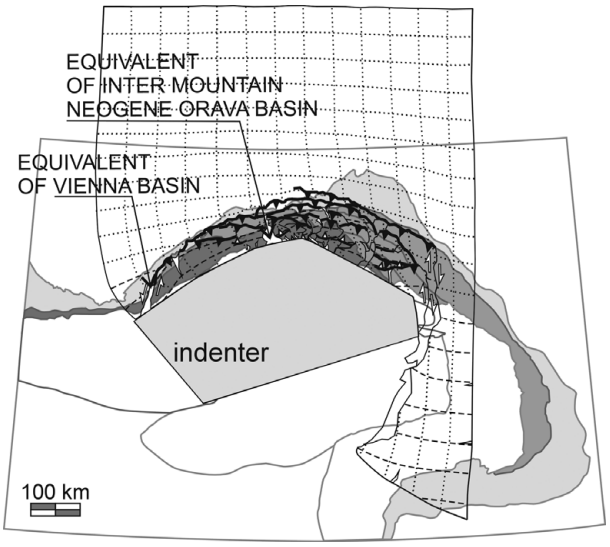

Figure 15. Comparison of the results of the third experiment (with quasi-triangular indenter which moved to the NE and simultaneously rotated anticlockwise; Fig. 13g) and the map-view of the Carpathian area (after Csontos *et al.* 1992). The figure shows the location of two significant gaps in the experimental prism which were located at a similar position as two Neogene basins of the Western Outer Carpathians.

counter-clockwise-rotating ALCAPA block which moved to the NE.

6. Summary and discussion of the modelling

The Outer Carpathian fold-and-thrust belt is one of the most curved belts in the world. The northern part of this belt was the subject of the present study. The curved thrust traces seen in map-view are common in real fold-and-thrust belts (e.g. Elliott, 1976; Fischer & Woodward, 1992). A variety of parameters generate curved fold-and-thrust belts (e.g. Butler *et al.* 1995; Macedo & Marshak, 1999; Yonkee & Weil, 2010). It is currently thought that the northern Outer Carpathian belt was formed as an accretionary prism in front of the advancing continental fragment, the so-called ALCAPA block during Oligocene–Miocene times (e.g. Pescatore & Ślączka 1984; Kováč *et al.* 1994; Morley 1996; Nemčok *et al.* 1998*a*; Fodor *et al.* 1999; Behrmann *et al*. 2000). The present-day southern boundary of the northern Outer Carpathians has a concave, quasi-triangular shape. The similar convex shape is the northern boundary of the northern Outer Carpathian belt, which suggests that the quasi-triangular ALCAPA block had an influence on the formation of the convexly curved Outer Carpathian belt; the influence of the indenter-controlled parameters was therefore tested at the beginning of this research. According to Macedo & Marshak (1999), the influence of indenter-controlled parameters on the generation of curved fold-and-thrust belts is indisputable. In order to test the possible influence of such parameters on the geodynamic evolution of the northern Outer Carpathian belt, three experiments which differed in respect of the shape of indenter used and its movement were conducted. The positive results of the modelling seem to be very promising, suggesting that it can be a plausible geodynamic analogue scenario for Oligocene–Miocene tectonic evolution of the northern Outer Carpathians. However, the positive results of modelling do not necessarily imply that other parameters are not important. For example, Nemčok *et al*. (1999) described the influence of basal friction on thrust generation in the Western Outer Carpathians. These authors suggested that the differences in basal friction influenced the formation of the Outer Carpathians. The models presented in this paper were simple; details of the tectonic evolution of this part of the Outer Carpathians should be investigated in successive experiments.

According to the results of the modelling, both the rectangular and triangular indenters caused the formation of experimental wedges which were more or less curved. The frontal indentation by the rectangular indenter of model 1 generated gently curved thrust traces in map-view and confirms previous experiments (e.g. Dixon & Liu, 1992). However, the experimental wedge in Experiment 1 was not curved enough in comparison to the real northern Outer Carpathian wedge (Fig. 8). According to literature, the wedges that were more curved were generated by indenters that had an angular outline to their leading edge (e.g. Davy & Cobbold, 1988; Zweigel, 1998, Lickorish *et al.* 2002) and the magnitude of wedge curvature depends on the magnitude of the curvature of the indenter (Marshak, 2004). The experimental shape of the ALCAPA block corresponded to the present southern margin of the Outer Carpathians, hence the choice of a quasi-triangular indenter shape so that the shape of the experimental wedge roughly mimics the shape of the indenter. The simple indentation of the quasi-triangular block northwards (in present geographic coordinates) produces a realistic wedge (Fig. 9a–e) and one that is roughly symmetrical, although this does not correspond to the asymmetry of the Western Outer Carpathian wedge (Fig. 12a). The two-stage model 2 (Fig. 12b) and model 3 (Fig. 15) are more suitable. However, none of these models exactly reproduces the geometry of the real orogen. In the two-stage model 2, the main thrusts were sharply terminated laterally and westwards on sinistral tear faults. In the western part of the Western Outer Carpathians, the main thrusts of the Magura and Silesian nappes were not so sharply terminated laterally on tear faults (Fig. 12a); these thrusts were possibly terminated on oblique thrusts as in model 3 (Fig. 15).

The northern Outer Carpathians were created as an accetionary prism, from hinterland to foreland, during the Late Eocene – Middle Miocene (Sarmatian) in front of the advancing ALCAPA block. The northern Outer Carpathian belt has a northwards convex outline, is asymmetric in shape and is wider at its eastern end (Fig. 1). The trend line of the basal thrusts of the main nappes is also convex to the north (with the exception

https://doi.org/10.1017/S0016756813000320 Published online by Cambridge University Press

of the Skole nappe which is exposed in the eastern part of the studied area).

In the fold-and-thrust model experiments reported here, wet sandy silt was used as the experimental material, a methodology based on the work of An & Sammis (1996), Mechelen (2004) and Eisenstadt & Sims (2005). A suitable water content for the degree of wetness was empirically determined by repeated testing.

At the start of indenter motion for all the models, the wet sandy silt took up the strain without visibly fracturing. Such an observation is in line with the results of the previous experiments, when the wet clay was an experimental material (Eisenstadt & Sims, 2005). The indenter movement at the start of an analogue experiment into wet clay does not cause the formation of macroscopically visible overthrusts.

The pressure of the indenter strained the experimental layer and produced a curving of the orthogonal grid in front of the moving indenter and simultaneous lateral escape of the material of the experimental layer (Figs 5b, 9b). Such an influence of the moving indenter on the foreland is less visible in experiment 3 with the rotated indenter (Fig. 13b). Latitudinal grid lines tended to compress within the experimental prism; longitudinal grid lines became curved and rotated counter-clockwise on the western part of the prism and clockwise on the eastern part, which is visible within all models.

Almost all the experimental prisms were characterized by greater or lesser rotations of the experimental material, as observed from the rotation of the grid lines. These rotations mainly depended on the magnitude of the indenter's curvature. In the model with the rectangular indenter, the rotation of the material within the experimental prism was very low and was located within the lateral ends of the frontal part of the prism. The well-marked opposite rotation of the material of the experimental wedge took place in front of the triangular indenter (Fig. 11a), suggested by the occurrence of the counter-clockwise rotation of the grid lines on the left-hand side of the indenter and the clockwise rotation on its right-hand side (in relation to the indenter's apex). Aleksandrowski (1989) and Nemčok *et al*. (2007) described a fan-shaped pattern for the stress axis σ_1 trajectories in the Polish part of the northern Outer Carpathian accretionary wedge (Magura and Silesian nappes).

The same phenomenon of opposite rotation of the experimental material appears in the model with rotating quasi-triangular indenter. In this case however, the counter-clockwise rotation of indenter increases the counter-clockwise rotation of the material in front of the left-hand side of the indenter, but decreases the clockwise rotation of the material in front of the right-hand side of indenter. The addition of a counter-clockwise rotation of the quasi-triangular indenter in experiment 3 therefore increased the counter-clockwise rotation of the experimental material in the western part of the experimental prism. In the eastern part of the prism however, the counter-clockwise rotation of the material (which was forced by indenter rotation) interfered with the clockwise rotation induced by having oblique indentation (Fig. 14a), reducing the amount of clockwise rotation of the experimental material within this part of wedge. Additionally, several slices seemed to be counter-clockwise rotated.

The same variability of the material rotation along the vertical axis, detected by palaeomagnetic investigation, is also observed in the northern Outer Carpathian belt. According to Grabowski *et al*. (2006), the amount of counter-clockwise rotation in the Silesian unit seems to decrease along-strike from SW to NE and E. Models 2 and 3 show the same trend (Figs 11, 14): the rotation value of the markers in the western part of the experimental wedge decreases along-strike from W to E up to the zone in front of the indenter apex.

Simple shearing could be inferred from rhomboid grid line development. When this occurred, the grid line rotation (Figs 5, 9, 13) cannot be simply taken as the equivalent of rotation in the real rocks as deduced palaeomagnetically.

In experiments 2 and 3 the southern slices in the central part of the experimental wedge were convexly bent to the North, and this geometry fits the Polish part of the northern Outer Carpathians. However, the main thrust in model 2 terminated westwards on tear faults. In the western part of the northern Outer Carpathians, only the trace line of the frontal thrust of the Magura nappe shows a stair-like geometry. This could mean that the Magura nappe, being the most southern/upper nappe of the studied wedge, was formed before the possible rotation of the ALCAPA block. That theory is consistent with the published information that the Magura nappe was attached to the ALCAPA block during the Oligocene (e.g. Oszczypko, 2006) and that this block started to rotate during the Miocene (e.g. Márton & Fodor, 2003).

The newly formed thrusts at the front of the prism in all experiments had a small curvature. The traces of thrusts dipping to the indenter were gently convex towards the foreland (e.g. Figs 9d, 13d; see the thrusts furthest from the indenter). At the beginning of the indentation, the strike of newly formed thrusts depended both on the indentation direction and the orientation of the indenter margin when indentation was oblique as in experiments 2 and 3 (Figs 9, 13). Later, the strike of new thrusts at the front of the prism was mostly dependent on indentation direction and was often not related to the shape of the indenter. As the experiments progressed, the indentation of the older innermost thrusts was accommodated to the indenter shape. The thrusts developed a greater degree of curvature within experiments 2 and 3 as compared to experiment 1 (Figs 5f, 9f, 13g). Such accommodation of the trend lines of the existing, older thrusts to the outline of the indenter has already been documented (e.g. Macedo & Marshak, 1999).

The major thrusts in all models were not linear; their geometry varied along-strike (Figs 5, 9, 13)

https://doi.org/10.1017/S0016756813000320 Published online by Cambridge University Press

as a result of the initial formation of separate segments that subsequently became linked along-strike as shortening increased. The major forward thrusts nucleated successively in sequence, and the majority of new thrusts were perpendicular, or near-perpendicular, to the shortening direction. The oblique thrusts in the models with the quasi-triangular indenter were an exception; they were numerous particularly at the beginning of the experiment. Their orientation depends on the relation between the orientation of the indenter margin and direction of indentation; such relationships have already been documented (Doglioni, 1992).

The orogen-parallel extension, manifested by stretching of the grid meshes, occurred in all experiments (Figs 5f, 9f, 13g). However, the occurrence of the tension gashes within the wedge is visible only in the case of the triangular-shaped indenter.

7. Comparison to the Western Alps

On a regional level, the main tectonic features of the northern Outer Carpathians have geometrical similarities to the Western Alps. The Western Alps developed during Cenozoic NW-directed collision of the Apulian microplate with the southwards-subducting European passive margin (Dewey *et al.* 1973; Vialon *et al.* 1989; Lickorish *et al.* 2002). Within the external Western Alps, two regional arcuate systems are distinguishable (Lickorish *et al.* 2002): (1) the structures of the Helvetic–Dauphinois zones, which form the older (Eocene–Miocene) internal and principal part of the Western Alps; and (2) the arcuate Jura arc and the Digne thrust, which form the younger (Miocene–Holocene) external part of this orogen. The internal Helvetic–Dauphinois system extends along the whole of the Western Alps, whereas the Jura belt is located at the right-hand side of this part of the Alps. The relative geometrical position of the Jura belt in relation to the Apulian microplate suggests a similarity to the position of the Skole nappe in the Western Outer Carpathians in relation to the ALCAPA block. A comparison of the Western Alps and the northern Outer Carpathians suggests that the Apulian microplate was more curved than the ALCAPA block, as the principal Western Alpine arc developed in two orthogonal and synchronous branches (Lickorish *et al.* 2002). According to Lickorish *et al*. (2002), from the Eocene to the Early Miocene the Apulian microplate moved along a slightly diagonal path with respect to the European margin. In the Middle Miocene, it then moved by counter-clockwise rotation of *c.* 10–15° along a curved path.

8. Conclusions

The experiments described here suggest that it is possible to reproduce the large-scale structures of the northern Outer Carpathians in two different ways using a quasi-triangular indenter: (1) in two successive directions varied by *c.* 45°, first to the north (in the present geographic coordinates) and then to the northeast; and (2) in one direction, to NE but with a simultaneous counter-clockwise rotation of *c.* 60°. Model 3, which incorporated counter-clockwise rotation of the indenter, produced results most similar to the northern Outer Carpathians.

The wet sandy silt used as experimental material meant that the influence of the indenter displacement was well-marked far outside the experimental prism. The pressure of the indenter strained the experimental layer and produced a curving of the orthogonal grid in front of the moving indenter and simultaneous lateral escape of the material in experiments 1 and 2 (Figs 5b, 9b). Such influence of the moving indenter on the foreland is less visible in experiment 3 with rotating indenter (Fig. 13b).

Rotation effects within the sandy silt experimental wedges were easily visible when the shape of the indenter was triangular. However, the occurrence of simple shearing means that the amount of experimental rotation and the amount of rotation in the actual orogen cannot be directly correlated. Counter-clockwise rotation of the indenter influences the model by increasing the counter-clockwise rotation of the slices in the western part of the experimental wedge and decreasing the clockwise rotation of the slices in its eastern part. When the amount of indenter rotation is large enough, the slices in the eastern part of the final model are also rotated counter-clockwise.

The results of the indentation modelling suggest that the orientation of the trace line of newly formed thrusts depends mostly on the indentation direction. At the start, all the thrusts (which dipped to the hinterland) were gently curved and were convex towards the foreland. When the indenter had straight margins the thrust traces became less curved, but when the indenter had a quasi-triangular shape the thrust traces became more curved because they accommodated more to the curvature of the indenter margin.

All three experiments produced a stack of scales equivalent to the development of an accretionary prism (Figs 5, 9, 13). The outline of all models was curved and this curvature depended principally on the curvature of the indenter. The least-curved model resulted from a rectangular-shaped indenter (Fig. 5f), while the most-curved model resulted from the use of the quasi-triangular-shaped indenter (Figs 9f, 13g). The quasi-triangular indenter produced a sufficiently curved experimental prism (model 2 and 3) to be comparable to that of the northern Outer Carpathians (Figs 12, 15), including the degree of prism asymmetry. Model 3 however, which incorporated indenter rotation, seemed to produce results most similar to the northern Outer Carpathians (Fig. 15).

According to the results of the experiments described here, the northern Outer Carpathians started to form when the ALCAPA block was moving approximately to the north (in relation to present position of the ALCAPA block) and had no significant rotation. The stair-like outline of the frontal thrust of the western

https://doi.org/10.1017/S0016756813000320 Published online by Cambridge University Press

part of Magura nappe suggests the occurrence of oblique thrusts or tear faults. Such faults were rare in the western part of the model when the indenter was rotated. The deformational front was later shifted to the Silesian nappe and the ALCAPA block started its counter-clockwise rotation during this time. This rotation probably finished with the formation of the Skole nappe.

Acknowledgements. This work was supported by the Ministry of Science and Higher Education (grant number NN 525363637) and the Institute of Geological Sciences, Polish Academy of Sciences (Karpaty, INGPAN). I would like to thank Tadeusz Kawiak (Institute of Geological Sciences, Polish Academy of Sciences) for mineral identifications, Dorota Bakowska and Małgorzata Zielińska (Institute of Geological Sciences, Polish Academy of Sciences) for measuring the density and water contents and Jacek Dąbrowski and Aleksandra Borecka (AGH University of Science and Technology, the Faculty of Geology, Geophysics and Environmental Protection) for analysing the mechanical and physical properties of the modelling material. I also thank anonymous reviewers for their constructive comments.

References

ALEKSANDROWSKI, P. 1985. Interference fold structure of the Western Flysch Carpathians in Poland. *13th Congress of the Carpatho-Balkan Geological Association*, 5–10th September 1985, Cracow, Proceeding Reports Part 1, 159–62.

ALEKSANDROWSKI, P. 1989. Geologia strukturalna płaszczowiny magurskiej w rejonie Babiej Góry [Structural geology of the Magura Nappe in the Mt. Babia Góra region, western Outer Carpathians]. *Studia Geologica Polonica* **96**, 1–140 (in Polish with English summary).

AN, L.-J. & SAMMIS, C. G. 1996. Development of strike-slip faults: shear experiments in granular materials and clay using a new technique. *Journal of Structural Geology* **18**, 1061–77.

BADA, G. 1999. *Cenozoic stress field evolution in the Pannonian Basin and surrounding orogens: Inferences from kinematic indicators and finite element modelling*. Published Ph.D. thesis, Vrije University, Amsterdam, 204 pp.

BALLA, Z. 1987. Tertiary paleomagnetic data for the Carpatho-Pannonian region in the light of Miocene rotation kinematics. *Tectonophysics* **139**, 67–98.

BEHRMANN, J. H., STASIANY, S., MILICKA, J. & PERESZLENYI, M. 2000. Quantitative reconstruction of orogenic convergence in the Northeast Carpathians. *Tectonophysics* **319**, 111–27.

BIRKENMAJER, K. 1986. Stages of structural evolution of the Pieniny Klippen Belt, Carpathians. *Studia Geologica Polonica* **80**, 7–32.

BOUTELIER, D., SCHRANK, C. & CRUDEN, A. 2008. Power-law viscous materials for analogue experiments: new data on the rheology of highly-filled silicone polymers. *Journal of Structural Geology* **30**, 341–53.

BRONIATOWSKA, M. 2008. Flysch massifs modelling and selection of parameters for slope stability calculations. *Czasopismo Techniczne*, 3–11. Wydawnictwo Politechniki Krakowskiej z. 1–Ś/2008, Biblioteka Cyfrowa PK (in Polish, with English summary).

BURCHFIL, B. C., 1980. Eastern European Alpine system and the Carpathian orocline as example of collision tectonics. *Tectonophysics* **63**, 31–61.

BUTLER, R. F., RICHARDS, D. R., SEMPERE, T. & MARSHALL, L. G. 1995. Paleomagnetic determinations of vertical-axis tectonic rotations from Late Cretaceous and Paleocene strata of Bolivia. *Geology* **23**, 799–802.

CALASSOU, S., LARROQUE, C. & MALAVIEILLE, J. 1993. Transfer zones of deformation in thrust wedges: an experimental study. *Tectonophysics* **221**, 325–44.

CHAPPLE, W. M. 1978. Mechanics of thin-skinned fold-and-thrust belts. *Geological Society of America Bulletin* **89**, 1189–98.

CHEN, C., LU, H., JI, D., CAI, D. & WU, S. 1999. Closing history of the southern Tianshan oceanic basin, western China: an oblique collisional orogeny. *Tectonophysics* **302**, 23–40.

COLLETTA, B., LETOUZEY, J., PINEDO, R., BALLARD, J. F. & BALÉ, P. 1991. Computerized X-ray tomography analysis of sandbox models: Examples of thin-skinned thrust systems. *Geology* **19**, 1063–7.

COTTON, J. T. & KOYI, H. A. 2000. Modeling of thrust fronts above ductile and frictional detachments: application to structures in the Salt Range and Potwar Plateau, Pakistan. *Geological Society of America Bulletin* **112**, 351–63.

CSONTOS, L. 1995. Tertiary tectonic evolution of the Intra-Carpathian area: a review. *Acta Vulcanologica* **7**, 1–13.

CSONTOS, L., NAGYMAROSY, A., HORVÁTH, F. & KOVÁČ, M. 1992. Tertiary evolution of the Intra-Carpathian area: a model. *Tectonophysics* **208**, 221–41.

CSONTOS, L. & VÖRÖS, A. 2004. Mesozoic plate tectonic reconstruction of the Carpathian region. *Palaeogeography, Palaeoclimatology, Palaeoecology* **210**, 1–56.

DAVIS, D., SUPPE, J. & DAHLEN, F. A. 1983. Mechanics of fold and thrust belts and accretionary wedges. *Journal of Geophysical Research* **88**, 1153–72.

DAVY, P. & COBBOLD, P. R. 1988. Indentation tectonics in nature and experiment. 1. Experiments scaled for gravity. *Bulletin of the Geological Institutions of the University of Uppsala*. New Series **14**, 129–41.

DECKER, K., NESCIERUK, P., REITER, F., RUBINKIEWICZ, J., RYŁKO, W. & TOKARSKI, A. K. 1997. Heteroaxial shortening, strike-slip faulting and displacement transfer in the Polish Carpathians. *Przegląd Geologiczny* **45**, 1070–1.

DECKER, K., TOKARSKI, A. K., JANKOWSKI, L., KOPCIOWSKI, R., NESCIERUK, P., RAUCH, M., REITER, F. & ŚWIERCZEWSKA, A. 1999. Structural development of Polish segment of the Outer Carpathians (Eastern part). Introduction to Stops: 7–16. *5th Carpathian Tectonic Workshop*, Poprad-Szymbark 5–9th June **1999**, 26–9.

DEWEY, J. F., PITMAN, W. C. (III), RYAN, W. B .F. & BONNIN, J. 1973. Plate tectonics and the evolution of the Alpine system. *Geological Society of America Bulletin* **84**, 3137–80.

DIXON, J. M. & LIU, S. 1992. Centrifuge modelling of the propagation of thrust faults. In *Thrust Tectonics* (ed. K. R. McClay), pp. 53–69. London: Chapman and Hall.

DOGLIONI, C. 1992. Main differences between thrust belts. *Terra Nova* **4**, 152–64.

EISENSTADT, G. & SIMS, D. 2005. Evaluating sand and clay models: do rheological differences matter? *Journal of Structural Geology* **27**, 1399–412.

ELLIOTT, D. 1976. The energy balance and deformation mechanisms of thrust sheets. *Philosophical Transactions of the Royal Society of London* **A 283**, 289–312.

ELLOUZE, N. & ROCA, E. 1994. Palinspastic reconstructions of the Carpathians and adjacent areas since the Cretaceous: a quantitative approach. In *Peri-Tethyan Platforms* (ed. F. Roure), pp. 51–78. Paris: Editions Technip.

FISCHER, M. P. & WOODWARD, N. B. 1992. The geometric evolution of foreland thrust systems. In *Thrust Tectonics* (ed. K. R. McClay), pp. 181–9. London: Chapman and Hall.

FODOR, L. 1995. From transpression to transtension Oligocene–Miocene tectonic evolution of the Vienna Basin and the East Alpine–Western Carpathian junction. *Tectonophysics* **242**, 151–82.

FODOR, L., CSONTOS, L., BADA, G., GYÖRFI, I. & BENKOVICS, L. 1999. Tertiary tectonic evolution of the Pannonian basin system and neighbouring orogens: a new synthesis of palaeostress data. In *The Mediterranean Basins: Tertiary Extension within the Alpine Orogen* (eds. B. Durand, L. Jolivet, F. Horváth, & M. Séranne), pp. 295–334. London: Geological Society, Special Publications **156**.

FODOR, L., MAGYARI, Á., KÁZMÉR, M. & FOGARASI, A. 1992. Gravity flow dominated sedimentation on the Buda paleoslope (Hungary): record of Late Eocene continental escape of the Bakony unit. *Geologische Rundschau* **81**, 695–716.

FRISCH, W., KUHLEMANN, J., DUNKL, I. & BRÜGEL, A. 1998. Palinspastic reconstruction and topographic evolution of the Eastern Alps during late Tertiary tectonic extrusion. *Tectonophysics* **297**, 1–15.

GOLONKA, J., OSZCZYPKO, N. & ŚLĄCZKA, A. 2000. Late Carboniferous-Neogene geodynamic evolution and paleogeography of the circum-Carpathian region and adjacent areas. *Annales Societatis Geologorum Poloniae* **70**, 107–36.

GRABOWSKI, J., KRZEMIŃSKI, L., NESCIERUK, P. & STARNAWSKA, E. 2006. Palaeomagnetism of the teschenitic rocks (Lower Cretaceous) in the Outer Western Carpathians of Poland: constraints for tectonic rotations in the Silesian unit. *Geophysical Journal International* **166**, 1077–94.

HEAD, K. H. 1992. *Manual of Soil Laboratory Testing. Volume 1: Soil Classification and Compaction Tests*. 2nd ed. Pentech Press London. pp. 761–5.

HUBBERT, M. K. 1937. Theory of scale models as applied to the study of geological structures. *Geological Society of America Bulletin* **48**, 1459–520.

HUBBERT, M. K. 1951. Mechanical basis for certain familiar geologic structures. *Geological Society of America Bulletin* **62**, 355–72.

JANKOWSKI, L. 1997. Warstwy z Gorlic - najmłodsze utwory południowej części jednostki śląskiej [Beds from Gorlice – the youngest strata of the southern part of the Silesian Unit]. *Przegląd Geologiczny* **45**, 305–8 (in Polish).

JANKOWSKI, L. 2007. Kompleksy chaotyczne w rejonie gorlickim (Polskie Karpaty Zewnętrzne) [Chaotic complexes in the Gorlice region (Polish Outer Carpathians)]. *Biuletyn Państwowego Instytutu Geologicznego* **426**, 27–52 (in Polish, with English summary).

KARNKOWSKI, P. 1974. Zapadlisko przedkarpackie – część wschodnia (na wschód od Krakowa) [Carpathian Foredeep – the eastern part (eastward from Cracow)]. In *Budowa Geologiczna Polski, Tektonika, Niż Polski*. (ed. W. Pożaryski), pp. 402–16.Wydawnictwo Geologiczne (in Polish).

KORÁB, T., KRS, M., KRSOVÁ, M. & PAGÁC, P. 1981. Paleomagnetic investigations of Albian(?)–Paleocene to Lower Oligocene sediments from the Dukla Unit, East Slovakian Flysch, Czechoslovakia. *Západné Karpaty, Geológia* **7**, 127–49.

KOTLARCZYK, J. 1985. An outline of the stratigraphy of Marginal Tectonic Units of the Carpathian orogen in the Kraków Przemyśl area. In *Geotraverse Kraków-Baranów-Rzeszów-Przemyśl-Komańcza-Dukla. XIII Congress Carpatho-Balkan Geological Association, Guide to Excursion 4* (ed. J. Kotlarczyk), pp. 21–32, Wydawnictwo Geologiczne, Warszawa.

KOVÁČ, M., KRÁL, J., MÁRTON, E., PLAŠIENKA, D. & UHER, P. 1994. Alpine uplift history of the Central Western Carpathians: geochronological, paleomagnetic, sedimentary and structural data. *Geologica Carpathica* **45**, 83–96.

KOVÁČ, M., NAGYMAROSY, A., OSZCZYPKO, N., ŚLĄCZKA, A., CSONTOS, L., MARUNTEANU, M., MATENCO, L. & MÁRTON, E. 1998. Palinspastic reconstruction of the Carpathian-Pannonian region during the Miocene. In *Geodynamic Development of the Western Carpathians* (ed. M. Rakuš), pp. 189–217. Slovak Geological Survey, Bratislava.

KRS, M., CHVOJKA, R. & POTFAJ, M. 1993. Paleomagnetic investigations in the Biele Karpaty Mts unit, flysch belt of the Western Carpathians. *Geologica Carpathica* **45**, 35–43.

KRS, M., KRSOVÁ, M., CHVOJKA, R. & POTFAJ, M. 1991. Paleomagnetic investigations of the flysch belt in the Orava region, Magura unit, Czechoslovak Western Carpathians. *Geologické Práce* **92**, 135–51.

KRS, M., KRSOVA, M. & PRUNER, P. 1996. Paleomagnetism and paleogeography of the Western Carpathians from the Permian to the Neogene. In *Paleomagnetism and Tectonics of the Mediterranean region* (eds A. Morris & D. H. Tarling) pp. 175–84. Geological Society of London, Special Publication no. 105.

KRS, M., MUSKA, P. & PAGÁČ, P. 1982. Review of paleomagnetic investigations in the West Carpathians of Czechoslovakia. *Geologické Práce* **78**, 39–58.

KRZYWIEC, P. 2001. Contrasting tectonic and sedimentary history of the central and eastern parts of the Polish Carpathian foredeep basin - results of seismic data interpretation. *Marine and Petroleum Geology* **18**, 13–38.

KSIĄŻKIEWICZ, M. 1977. The tectonics of the Carpathians. In: *Geology of Poland. Volume 4: Tectonics*, pp. 476–669. Geological Institute, Warszawa.

LEXA, O., SCHULMANN, K. & JEŽEK, J. 2003. Cretaceous collision and indentation in the West Carpathians: view based on structural analysis and numerical modeling. *Tectonics* **22**, 1066, doi:10.1029/2002TC001472

LEXA, V., ELECKO, M., MELLO, J., POLAK, M., POTFAJ, M. & VOZAR, J. (eds) 2000. *Geological Map of Western Carpathians and Adjacent Areas 1:500 000*. Geological Survey of Slovenia, Bratislava.

LICKORISH, W. H., FORD, M., BÜRGISSER, J., & COBBOLD, P. 2002. Arcuate thrust systems produced by sand-box modelling: a comparison to the external arc of the Western Alps. *Geological Society of America Bulletin* **114**, 1089–107.

LIU, H., MCCLAY, K. R. & POWELL, D. 1992. Physical models of thrust wedges. In *Thrust Tectonics* (ed. K. R. McClay), pp. 71–81. London: Chapman and Hall.

ŁUKASZEWICZ, P., 2007. Deformational properties of flysch sandstones under conventional triaxial compressions. *Archives of Mining Sciences*, **52**, 371–85.

MACEDO, J. & MARSHAK, S. 1999. Controls on the geometry of fold-thrust belt salients. *Geological Society of America Bulletin* **111**, 1808–22.

MARSHAK, S. 2004. Salients, recesses, arcs, oroclines, and syntaxes; a review of ideas concerning the formation of map-view curves in fold-thrust belts. In *Thrust Tectonics and Hydrocarbon Systems* (ed. K. R. McClay), pp. 131–56. American Association of Petroleum Geologists, Memoir 82.

MARSHAK, S. & WILKERSON, M.S. 1992. Effect of overburden thickness on thrust belt geometry and development. *Tectonics* **11**, 560–6.

MÁRTON, E. & FODOR, L. 2003. Tertiary paleomagnetic results and structural analysis from the Transdanubian Range (Hungary): rotational disintegration of the Alcapa unit, *Tectonophysics* **363**, 201–24.

MÁRTON, E., KUHLEMANN, J., FRISCH, W. & DUNKL, I. 2000. Miocene rotations in the Eastern Alps—Paleomagnetic results from intramontane basin sediments. *Tectonophysics* **323**, 163–82.

MÁRTON, E. & MÁRTON, P. 1996. Large scale rotation in North Hungary during the Neogene as indicated by paleomagnetic data. In *Paleomagnetism and Tectonics of the Mediterranean Region* (eds A. Morris & D. H. Tarling), pp. 153–73. Geological Society of London, Special Publication no. 105.

MÁRTON, E., MASTELLA, L. & TOKARSKI, A. K. 1999. Large counterclockwise rotation of the Inner West Carpathian Paleogene Flysch—evidence from paleomagnetic investigation of the Podhale Flysch (Poland). *Physics and Chemistry of the Earth (A)* **24**, 645–9.

MÁRTON, E., RAUCH-WŁODARSKA, M., KREJČÍ, O., TOKARSKI, A. K. & BUBÍK, M. 2009. An integrated palaeomagnetic and AMS study of the Tertiary flysch from the OuterWestern Carpathians. *Geophysical Journal International* **177**, 925–40.

MÁRTON, E., TISCHLER, M., CSONTOS, L., FÜGENSCHUH, B. & SCHMID, S. M. 2007. The contact zone between the ALCAPA and Tisza-Dacia megatectonic units of Northern Romania in the light of new paleomagnetic data. *Swiss Journal of Geosciences* **100**, 109–24.

MÁRTON, E., TOKARSKI, A. K., KREJČÍ, O., RAUCH, M., OLSZEWSKA, B., TOMANOVÁ, P. & WÓJCIK, A. 2011. 'Non-European' palaeomagnetic directions from the Carpathian Foredeep at the southern margin of the European plate. *Terra Nova* **23**, 134–44.

MASTELLA, L. & KONON, A. 2002. Jointing in the Silesian Nappe (Outer Carpathians, Poland—Palaeostress reconstruction). *Geologica Carpathica* **53**, 315–25.

MATENCO, L. & BERTOTTI, G. 2000. Tertiary tectonic evolution of the external East Carpathians (Romania). *Tectonophysics* **316**, 255–86.

MECHELEN, J. L. M. 2004. Strength of moist sand controlled by surface tension for tectonic analogue modeling. *Tectonophysics* **384**, 275–84.

MORLEY, C. K. 1996. Models for relative motion of crustal blocks within the Carpathian region, based on restorations of the outer Carpathian thrust sheets. *Tectonics* **15**, 885–904.

MULUGETA, G. 1988. Modelling the geometry of Coulomb thrust wedges. *Journal of Structural Geology* **10**, 847–59.

MULUGETA, G. & KOYI, H. 1987. Three-dimensional geometry and kinematics of experimental piggyback thrusting. *Geology* **15**, 1052–6.

MULUGETA, G. & KOYI, H. 1992. Episodic accretion and strain partitioning in a model sand wedge. *Tectonophysics* **202**, 319–33.

NEMČOK, M., COWARD, M. P., SECOMBE, W. J. & KLECKER, R. A. 1999. Structure of the West Carpathian accretionary wedge: Insights from cross section construction and sandbox validation. *Physics and Chemistry of the Earth (A)* **24**, 659–65.

NEMČOK, M., DILOV, T., WOJTASZEK, M., LUDHOVÁ, L., KLECKER, R. A., SERCOMBE, W. J. & COWARD, M. P. 2007. Dynamics of the Polish and Eastern Slovakian parts of the Carpathian accretionary wedge: insights from palaeostress analyses. In *Deformation of the Continental Crust: The Legacy of Mike Coward* (eds A. C. Ries, R. W. H. Butler & R. H. Graham), pp. 271–302. Geological Society of London, Special Publication no. 272.

NEMČOK, M., HOUGHTON, J. J. & COWARD, M. P. 1998*a*. Strain partitioning along the western margin of the Carpathians. *Tectonophysics* **292**, 119–43.

NEMČOK, M., KRZYWIEC, P., WOJTASZEK, M., LUDHOVÁ, L., KLECKER, R. A., SERCOMBE, W. J. & COWARD, M. P. 2006. Tertiary development of the Polish and eastern Slovak part of the Carpathian accretionary wedge: insights from balanced cross-sections. *Geologica Carpathica* **57**, 355–70.

NEMČOK, M. & NEMČOK, J. 1994. Late Cretaceous deformation of the Pieniny Klippen Belt, Western Carpathians. *Tectonophysics* **239**, 81–109.

NEMČOK, M., POSPIŠIL, L., LEXA, J. & DONELICK, R. A. 1998*b*. Tertiary subduction and slab break-off model of the Carpathian-Pannonian region. *Tectonophysics* **295**, 307–40.

NEUGEBAUER, J., GREINER, B., & APPEL, E. 2001. Kinematics of the Alpine-West Carpathian orogen and paleogeographic implications. *Journal of the Geological Society, London* **158**, 97–110.

O'BRIEN, P. J. 2001. Subduction followed by collision: Alpine and Himalayan examples. *Physics of the Earth and Planetary Interiors* **127**, 277–91.

OLSZEWSKA, B. 1999. Biostratygrafia neogenu zapadliska przedkarpackiego w świetle nowych danych mikropaleontologicznych [Neogene biostratigraphy of the Carpathian Foredeep in light of the new micropaleontological data]. *Prace Państwowego Instytutu Geologicznego* CLXVIII, 9–28 (in Polish).

OSZCZYPKO, N. 1998. The Western Carpathian Foredeep - development of the foreland basin in front of the accretionary wedge and its burial history (Poland). *Geologica Carpathica* **49**, 415–31.

OSZCZYPKO, N. 2004. The structural position and tectonosedimentary evolution of the Polish Outer Carpathians. *Przegląd Geologiczny* **52**, 780–91.

OSZCZYPKO, N. 2006. Late Jurassic–Miocene evolution of the Outer Carpathian fold-and-thrust belt and its foredeep basin (Western Carpathians, Poland). *Geological Quarterly* **50**, 169–94.

PESCATORE, T. & ŚLĄCZKA, A. 1984. Evolution models of two flysch basins: the Northern Carpathians and Southern Appennines. *Tectonophysics* **106**, 49–70.

PETTIJOHN, F. J. 1975. *Sedimentary Rocks*. Third edition. New York: Harper and Row Publishers Inc. 628 pp.

PICHA, F., STRÁNÍK, Z. & KREJČÍ, O. 2005. Geology and hydrocarbon resources of the Outer Western Carpathians and their foreland, Czech Republic. In *The Carpathians and their Foreland: Geology and Hydrocarbon Resources* (eds J. Golonka & F. Picha), pp. 49–175.

American Association of Petroleum Geologists, Memoir 84.

PLAŠIENKA, D. 1991. Mesozoic tectonic evolution of the epi-Variscan continental crust of the Western Carpathians: A tentative model. *Mineralia Slovaca* **23**, 447–57.

PLAŠIENKA, D. P., GRECULA, M., PUTIŠ, M., KOVÁČ. & HOVORKA, D. 1997. Evolution and structure of the Western Carpathians: an overview. In *Geological Evolution of the Western Carpathians* (eds P. Grecula, D. Hovorka & M. Putiš), pp. 1–24, Mineralia Slovaca, Monograph, Bratislava.

POŁTOWICZ, S. 1991. Miocen strefy karpackiej między Wieliczką a Dębicą [Miocene of the Carpathian zone between Wieliczka and Dębica]. *Zeszyty Naukowe AGH Geologia* **17**, 19–57 (in Polish, with English summary).

POPRAWA, P., MALATA, T. & OSZCZYPKO, N. 2002. Ewolucja tektoniczna basenów sedymentacyjnych polskiej części Karpat zewnętrznych w świetle analizy subsydencji [Tectonic evolution of sedimentary basins of the Polish part of the Outer Carpathians in the light of subsidence analysis] *Przegląd Geologiczny* **11**, 1092–108 (in Polish).

POWDERS, M. C. 1953. A new roundness scale for sedimentary particles. *Journal of Sedimentary Petrology* **23**, 117–9.

RAUCH, M. 2001. Evolution of the Polish segment of the Western Outer Carpathians forced by the Tertiary convergence of the ALCAPA. The results of laboratory modelling. In: *Abstracts of the Carpathian Petroleum Conference 'Application of modern exploration methods in a complex petroleum system' Wysowa, June 2001* (ed. P. Dziadzio), pp. 82–87.

RATSCHBACHER, L., FRISCH, W., LINZER, H. G. & MERLE, O. 1991*a*. Lateral extrusion in the Eastern Alps: Part 2. Structural analysis. *Tectonics* **10**, 257–71.

RATSCHBACHER, L., FRISCH, W., LINZER, H. G., SPERNER, B., MESCHEDE, M., DECKER, K., NEMČOK, M., NEMČOK, J. & GRYGAR, R. 1993. The Pieniny Klippen Belt in the Western Carpathians of northeastern Slovakia, structural evidence for transpression. *Tectonophysics* **226**, 471–83.

RATSCHBACHER, L., MERLE, O., DAVY, P. & COBBOLD, P. 1991*b*. Lateral extrusion in the Eastern Alps: Part 1. Boundary conditions and experiments scaled for gravity. *Tectonics* **10**, 245–56.

REITER, K., KUKOWSKI, N. & RATSCHBACHER, L. 2011. The interaction of two indenters in analogue experiments and implications for curved fold-and-thrust belts. *Earth and Planetary Science Letters* **302**, 132–46.

ROCA, E., BESSEREAU, G., JAWOR, E., KOTARBA, M. & ROURE, F. 1995. Pre-Neogene evolution of the Western Carpathians: constraints from the Bochnia-Tatra Mountains section (Polish Western Carpathians). *Tectonics* **14**, 855–73.

ROYDEN, L. H. 1993. Evolution of retreating subduction boundaries formed during continental collision. *Tectonics* **12**, 629–38.

ROYDEN, L. H. & BURCHFIELD, B. C. 1989. Are systematic variations in thrust belt style related to plate boundary processes? (The Western Alps versus the Carpathians). *Tectonics* **8**, 51–61.

RUBINKIEWICZ, J. 2000. Development of fault pattern in the Silesian nappe: Eastern Outer Carpathians, Poland. *Geological Quarterly* **44**, 391–403.

SCHELLART, W. P. 2000. Shear test results for cohesion and friction coefficients for different granular materials: scaling implications for their usage in analogue modelling. *Tectonophysics* **324**, 1–16.

SCHMID, S. M., AEBLI, H. R., HELLER, F. & ZINGG, A. 1989. The role of the Periadriatic line in the tectonic evolution of the Alps. In *Alpine Tectonics* (ed. M. P. Coward), pp. 153–171. Geological Society of London, Special Publication no. 45.

SCHMID, S. M., BERNOULLI, D., FÜGENSCHUH, B., MATENCO, L., SCHEFER, S., SCHUSTER, R., TISCHLER, M. & USTASZEWSKI, K. 2008. The Alpine-Carpathian-Dinaridic orogenic system: correlation and evolution of tectonic units. *Swiss Journal of Geosciences* **101**, 139–83.

SIENIAWSKA, I., ALEKSANDROWSKI, P., RAUCH, M. A. & KOYI, H. 2010. Control of synorogenic sedimentation on back and out-of-sequence thrusting: insights from analog modeling of an orogenic front (Outer Carpathians, southern Poland). *Tectonics* **29**, TC6012.

ŚLĄCZKA, A., KRUGŁOV, S., GOLONKA, J., OSZCZYPKO, N. & POPADYUK, I. 2005. Geology and hydrocarbon resources of the Outer Carpathians, Poland, Slovakia, and Ukraine: general geology. In *The Carpathians and their Foreland: Geology and Hydrocarbon Resources* (eds J. Golonka & F. J. Picha), p. 221–58. American Association of Petroleum Geologists, Memoir 84.

SPERNER, B., RATSCHBACHER, L. & NEMČOK, M. 2002. Interplay between subduction rollback and lateral extrusion, tectonics of the Western Carpathians. *Tectonics* **21**, 1051–75.

STEFANIUK, M., OSTROWSKI, C., TARGOSZ, P., WOJDYŁA, M. 2009. Some problems of magnetotelluric and gravity structural investigations in the Polish Eastern Carpathians. *Geologia* **4**, 7–46, Wydawnictwo AGH, Kraków (in Polish, with English summary).

ŚWIERCZEWSKA, A. & TOKARSKI, A. K. 1998. Deformation bands and the history of folding in the Magura nappe, Western Outer Carpathians (Poland). *Tectonophysics* **297**, 73–90.

TAPPONNIER, P., PELTZER, G., LE DAIN, A. Y. & ARMIJO, R. 1982. Propagating extrusion tectonics in Asia: New insights from simple experiments with plasticine. *Geology* **10**, 611–6.

TOKARSKI, A. K., ŚWIERCZEWSKA, A., ZUCHIEWICZ, W., MÁRTON, E., HURAI, V., ANCZKIEWICZ, A., MICHALIK, M., SZELIGA, W. & RAUCH-WŁODARSKA, M. 2006. Structural development of the Magura Nappe (Outer Carpathians): from subduction to collapse. *Geolines* **20**, 145–64.

USTASZEWSKI, K., SCHMID, S. M., FÜGENSCHUH, B., TISCHLER, M., KISSLING, E. & SPAKMAN, W. 2008. A map-view restoration of the Alpine-Carpathian-Dinaridic system for the Early Miocene. *Swiss Journal of Geosciences* **101**, S273–S294 Supplement 1.

VIALON, P., ROCHETTE, P. & MENARD, G. 1989. Indentation and rotation in the western Alpine arc. In *Alpine Tectonics* (eds M. P. Coward, D. Dietrich & R. G. Park), pp. 329–38. Geological Society of London, Special Publication no. 45.

WÓJCIK, A., SZYDŁO, A., MARCINIEC, P., & NESCIERUK, P. 1999. The folded Miocene of the Andrychów region. *Biuletyn Państwowego Instytutu Geologicznego* **387**, 191–5.

YONKEE, A. & WEIL, A. B. 2010. Reconstructing the kinematic evolution of curved mountain belts: Internal strain patterns in the Wyoming salient, Sevier thrust belt, U.S.A. *Geological Society of America Bulletin* **122**, 24–49.

ZUCHIEWICZ, W., TOKARSKI, A. K., JAROSIŃSKI, M. & MÁRTON, E. 2002. Late Miocene to present day structural development of the Polish segment of the Outer Carpathians. *Stephan Mueller Special Publication* **3**, 185–202.

ZWEIGEL, P. 1998. Arcuate accretionary wedge formation at convex plate margin corners: results of sandbox analogue experiments. *Journal of Structural Geology* **20**, 1597–609.

ŻYTKO, K., GUCIK, S., RYŁKO, W., OSZCZYPKO, N., ZAJĄC, R., GARLICKA, I., NEMČOK, J., ELIÁŠ, M., MENČÍK, E., DVOŘÁK, J., STRÁNÍK, Z., RAKUS, M. & MATEJOVSKÁ, O. 1989. Geological map of the Western Outer Carpathians and their foreland without Quaternary formations. In *Geological Atlas of the Western Outer Carpathians and their Foreland*. (eds D. Poprawa & J. Nemčok). Wydawnictwo Państwowego Instytutu Geologicznego, Warszawa.

https://doi.org/10.1017/S0016756813000320 Published online by Cambridge University Press